Article

Current Biology

# The origin and evolution of dorsal determination mechanisms in vertebrate paired appendages

## Highlights

- Lmx1b is a primary genetic determinant of dorsal identity in limbs and paired fins
- A conserved regulatory hub, the *LARM*, drives appendage-specific Lmx1b expression
- *LARM* control of Lmx1b is a paired fin innovation and is not deployed in median fins
- Variation in *LARM* sequences underlies adaptive changes in dorsal-ventral fin anatomy

## Authors

M. Brent Hawkins, Sofía Zdral, Silvia Naranjo, ..., Matthew P. Harris, Juan J. Tena, Marian A. Ros

## Correspondence

harris@genetics.med.harvard.edu (M.P.H.), marian.ros@unican.es (M.A.R.)

## In brief

Limbs have distinct sidedness, with dorsal-ventral flexure allowing diverse movements that permit nuanced articulation and function. Hawkins et al. demonstrate that the genetic foundation of this patterning is an ancestral feature of paired fins, predating the fin-to-limb transition. Further, they detail how variation in this regulation underlies adaptive morphological change.

Hawkins et al., 2026, Current Biology *36*, 1–13
July 6, 2026 
https://doi.org/10.1016/j.cub.2026.05.046

CellPress

Current Biology

CellPress
OPEN ACCESS

Article

# The origin and evolution of dorsal determination mechanisms in vertebrate paired appendages

M. Brent Hawkins,[1,2,10] Sofía Zdral,[3,10] Silvia Naranjo,[4] Miguel Juliá,[3] Manuel Sánchez-Martín,[5] Jacob M. Daane,[6] Nicolás Cumplido,[7] David Jandzik,[8] Daniel M. Medeiros,[9] Sarah K. McMenamin,[7] Matthew P. Harris,[1,2,11,12,*] Juan J. Tena,[4,11] and Marian A. Ros[3,11,*]

[1]Boston Children's Hospital, Department of Orthopedic Research, Boston, MA 02115, USA
[2]Harvard Medical School, Department of Genetics, Boston, MA 02115, USA
[3]Instituto de Biotecnología y Biomedicina de Cantabria, CSIC-SODERCAN-Universidad de Cantabria, 39005 Santander, Spain
[4]Centro Andaluz de Biología de Desarrollo, CSIC-Universidad Pablo de Olavide, 41013 Seville, Spain
[5]Institute of Biomedical Research of Salamanca (IBSAL), Universidad de Salamanca, 37008 Salamanca, Spain
[6]Department of Biology and Biochemistry, University of Houston, Houston, TX 77004, USA
[7]Biology Department, Boston College, Chestnut Hill, MA 02467, USA
[8]Department of Zoology, Comenius University, 814 99 Bratislava, Slovakia
[9]Department of Ecology and Evolutionary Biology, University of Colorado, Boulder, CO 80309, USA
[10]These authors contributed equally
[11]Senior author
[12]Lead contact
*Correspondence: harris@genetics.med.harvard.edu (M.P.H.), marian.ros@unican.es (M.A.R.)
https://doi.org/10.1016/j.cub.2026.05.046

## SUMMARY

Limb function requires polarized anatomy across the dorsal-ventral axis, but it is unclear when the capacity for differentiation along this axis in paired appendages arose during vertebrate evolution. Here, we define ancestral dorsoventral patterning programs in the fins of fishes. We show that an ortholog of the limb dorsal determinant, Lmx1b, is required to establish dorsality in zebrafish pectoral fins and is activated by a conserved jawed vertebrate *cis*-regulatory hub. However, this hub is not essential for *lmx1bb* expression in median fins, suggesting that this control is an evolutionary innovation specific to the paired appendages. Although we find that the regulatory hub is highly conserved across gnathostomes, we identify a specific alteration of this region in hillstream loaches, fishes that naturally parallel the "double-ventral" fin phenotypes observed in zebrafish *lmx1bb* regulatory mutants. Altogether, our findings indicate that specific regulation of dorsal identity is an ancestral feature of paired appendage development that provided a prepattern for limb evolution and lineage diversification.

## INTRODUCTION

The evolutionary transition from fins into limbs involved integrated anatomical transformations along the proximal-distal (PD), anterior-posterior (AP), and dorsal-ventral (DV) axes. Although differences between fin and limb skeletons are dramatic along the PD (shoulder to finger) and AP (thumb to pinky) axes, the extent of DV morphological diversity (back of the hand to palm, Figure 1A) remains to be detailed, despite being critical for limb function.[1] The correct arrangement of internal elements, such as flexor and extensor muscles, and superficial structures, such as hair, nails, pads, and glands, on the dorsal and ventral aspects of the limb is required to enable movement, articulation, and sensory functions. Thus, the limited investigation into the regulation and diversification of this axis during appendage development and evolution may be masking important nodes of morphological change.

The existence of DV polarized anatomy is less apparent in fins than in limbs, and it is unknown whether and how DV polarity is developmentally informed in fins. It is possible that such patterning mechanisms are shared between fins and limbs due to their derivation from a common antecedent appendage or, alternatively, could be a limb-specific feature. A recent indication of morphological DV asymmetry in the fin rays of tetrapodomorph fish fossils, which are windows into the early skeletal transitions of limb-harboring vertebrates, suggests that DV patterning mechanisms existed prior to the emergence of limbs.[2] It remains unclear whether such cues are shared with ray-finned fishes and other jawed vertebrates.

The identification of molecular factors that establish DV polarity in the developing limb was achieved through seminal experimental studies in mouse and chicken[3–7] (Figure 1B). Of the known genetic regulators, Lmx1b is both necessary and sufficient for the formation of limb tissue with dorsal identity, whereas ventral identity is considered a default state.[3–5] Loss of *Lmx1b* function in the mouse results in an anatomically mirrored double-ventral phenotype in the distal limb, wherein ventral features develop on the dorsal aspect, while dorsal structures such as hair and nails are reduced or absent.[8,9] Reciprocally, loss of En1 activity in the ventral ectoderm causes a "double-dorsal"

Please cite this article in press as: Hawkins et al., The origin and evolution of dorsal determination mechanisms in vertebrate paired appendages, Current Biology (2026), https://doi.org/10.1016/j.cub.2026.05.046



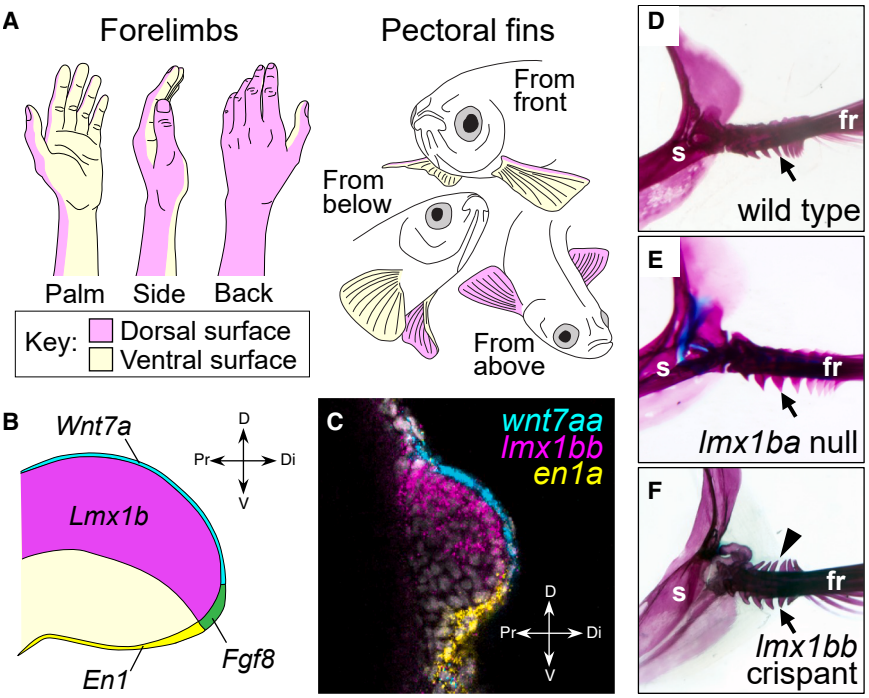


**Figure 1. Dorsal specification is functionally conserved in limb and paired fin development**

(A) Schematic indicating the dorsal (magenta) and ventral (yellow) regions of paired appendages.

(B) Diagram of DV patterning gene expression domains in the developing limb bud.

(C) 36 hpf zebrafish pectoral fin buds express DV patterning gene orthologs in domains conserved with limbs.

(D) Wild-type adult zebrafish pectoral fin skeleton stained with Alizarin Red (for bone) and Alcian Blue (for cartilage) exhibiting fin ray flanges restricted to the ventral aspect (black arrow, $n$ = 10).

(E) Null *lmx1ba* mutants have wild-type fin anatomy ($n$ = 10).

(F) *lmx1bb* crispant fins express a double-ventral phenotype with ectopic dorsal flanges (black arrowhead). In 45 adult *lmx1bb* crispant fish, fin ventralization was unilateral in 13 individuals and bilateral in 15 individuals. Dorsal to top, distal to right in (B)–(F). D, dorsal; di, distal; fr, fin rays; pr, proximal; s, scapulocoracoid; v, ventral.

See also Figures S1 and S2 and Table S1.

phenotype at distal levels of the limb, resulting in dorsal structures developing on the ventral side.[7,10]

Recent studies have identified the gene regulatory architecture that controls *Lmx1b* transcription specifically in the developing mouse limb. After initial activation by Wnt7a and other signals from the dorsal limb ectoderm, *Lmx1b* in the dorsal mesenchyme maintains its own expression through the binding of two upstream autoregulatory elements (Figure 2A), called *Lmx1b*-associated *cis*-regulatory modules 1 and 2 (*LARM1* and *LARM2*).[1,11] Based on reporter assays in chicken embryos, *LARM1* can be divided into two elements: a putative silencer sequence (*LARM1s*) and an enhancer region (*LARM1e*). Targeted removal of all *LARM* elements (*ΔLARM1/2*, 7.6 kb) in mice recapitulates the double-ventral phenotype of *Lmx1b* loss of function.[1] The limbs of these mutants are incapable of lifting the body due to ventralization of dorsal muscular elements and severe joint malformations, demonstrating that proper DV polarity is essential for limb-based locomotion. Although initial comparative bioinformatic analysis found that the *LARM* is highly conserved across tetrapods and lobe-finned fishes, orthologs in other branches of vertebrate phylogeny were not readily identified by conventional sequence conservation analyses.[1]

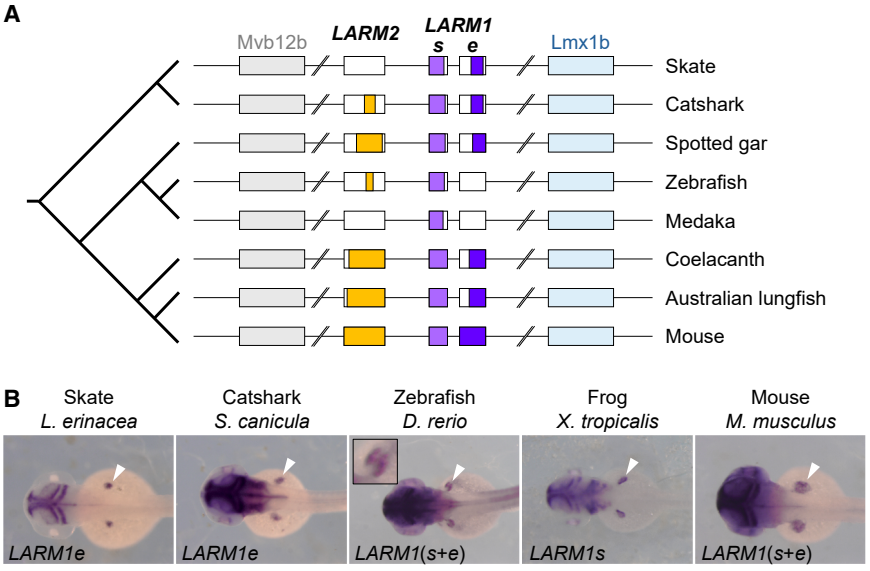


**Figure 2. The regulatory hub that controls dorsal limb *Lmx1b* expression is conserved across jawed vertebrates**

(A) Schematic of the *Mvb12b-Lmx1b* intergenic region containing the *LARM* elements. Colored region in each box represents extent of sequence conservation revealed by the lobe-finned HMM model (*bb* paralog shown for medaka and zebrafish). Diagonal hatched lines indicate omitted DNA regions and denote that the schematic is not drawn to scale.

(B) *In situ* hybridization of GFP transcripts in stable zebrafish $F_1$ reporter transgenics at 48 hpf shows *LARM* elements from various donor gnathostome species (named above each panel) drive expression in the pectoral fin (white arrowheads, magnified in inset) in transgenic assays. Dorsal view, anterior to left in (B). LARM sequences used are presented in Table S2.

See also Figures S3 and S4 and Table S1.

Although the presence of DV polarized morphology and its genetic regulation have been well described in the amniote limb, it is unclear whether and how such patterning is established and modified in the development of fins. Here, we describe anatomical DV polarity of paired fins in the zebrafish (*Danio rerio*) and experimentally assess genetic regulation of dorsal and ventral fate, comparing activity of teleost-specific orthologs of factors known to control DV specification in the chick and mouse. We reveal broad conservation of DV patterning mechanisms in developing paired appendages as well as identify their ancient gnathostome-specific origin. Additionally, we uncover *LARM* element functionality that is shared across vertebrate paired appendages but is absent from median fins. Against this background of evolutionary conservation, we highlight the association of natural variation in *LARM* domains with adaptive anatomical changes in certain teleost lineages harboring pectoral fin elaborations that mirror double-ventral phenotypes. This lineage-specific variation in loaches is the first indication of adaptive DV alteration in skeletal patterning and provides a clear genomic signature of alteration in the *LARM* regulatory hub.

## RESULTS

### A dorsal determinant program shared across fins and limbs

Mouse and chick limb buds express patterning factors of DV specification within conserved domains during development (Figure 1B), with *Wnt7a* in the dorsal epithelium subtended by *Lmx1b* in the dorsal mesenchyme and *En1* in the ventral ectoderm.[3–5,12] To assess similarities in temporal and spatial expression of fish orthologs of these factors, we performed hybridization chain reaction (HCR) RNA-fluorescence *in situ* hybridization (FISH) in the developing fin buds of zebrafish embryos. At 36 hours post-fertilization (hpf), a stage comparable to early budding limbs, orthologs of these genes, *wnt7aa*, *lmx1bb*, and *en1a*, are expressed in domains conserved in mouse and chick (Figure 1C). These results agree with previous reports of polarized expression in zebrafish.[13–17] Because *lmx1bb* has been reported in the adductor muscle of the zebrafish pectoral fin bud,[17] whereas in mouse *Lmx1b* is restricted to lateral plate mesoderm derivatives and excluded from the muscle lineage,[18] we asked whether the expression domains of *Lmx1b* orthologs differ between species. Probes for *lmx1bb* and two muscle lineage markers, *lbx1b*[19] and *pax3a*,[20,21] revealed non-overlapping expression in fins, supporting conserved mesenchymal-specific expression of *lmx1bb* in fins as in limbs (Figure S1).

### Functional integration of dorsal fate regulation in zebrafish

To determine whether these genes share a conserved function in the DV patterning of the fin, we used CRISPR-Cas9 to generate loss-of-function alleles of the zebrafish orthologs of *En1* (*en1a* and *en1b*) and *Lmx1b* (*lmx1ba* and *lmx1bb*) and analyzed their effect on fin anatomy. Wild-type pectoral fins display DV asymmetry, developing bony flanges only on the ventral side (Figure 1D). Consistent with the observation that *lmx1ba* is not detected in zebrafish pectoral fin buds,[22] homozygous mutants for *lmx1ba* are phenotypically wild type (Figure 1E). However, *lmx1bb* crispants show a dramatic double-ventral fin phenotype in which the dorsal aspect of the pectoral fin is transformed to develop ventral anatomy, including formation of the bony flanges (Figure 1F). This phenotype parallels the double-ventral limbs of *Lmx1b*-null mice.[8] Similar to the neonatal lethality observed in *Lmx1b*-null mutants, homozygous loss of function of *lmx1bb* is incompatible with viability past larval stages in the zebrafish,[23] presumably due to the pleiotropic functions of Lmx1b, preventing assessment of the adult fin phenotype in these coding mutants. Our results demonstrate that, as in limbs, Lmx1b is required to establish dorsal specification. This function is retained in the *lmx1bb* paralog, as *lmx1ba* loss of function does not have a discernible fin phenotype nor is it able to complement the loss of *lmx1bb*.

As En1 has been shown to dorsally restrict *Wnt7a* and *Lmx1b* expression in amniote limbs, we asked whether this genetic interplay at the core of DV axis patterning is also observed during fin development. Zebrafish *en1a*;*en1b* double-null animals are adult viable and express a pigment patterning phenotype (Figure S2B). In contrast to the *En1* knockout mouse limb, we do not observe a dorsalization phenotype in the *en1;en1b*-deficient zebrafish fin (Figure S2D). As the ventral fin surface does not have obvious polarized structures apart from the proximal flanges, changes in more distal fates in the fin cannot be scored. In mouse, loss of *En1* function results in the activation of *Wnt7a* expression in the ventral ectoderm,[7] which, in turn, induces ectopic *Lmx1b* expression in the ventral mesenchyme. Similarly, *en1a*;*en1b* mutant fins exhibit ectopic ventral expression of *wnt7aa* and *lmx1bb* transcripts (Figure S2H). Altogether, our results demonstrate that the integrated signaling network of DV specification as defined in mouse limb is intact and functionally conserved in zebrafish pectoral fins.

### Ancestral origin and evolutionary conservation of *Lmx1b* regulatory elements

Given the conserved interactions between DV patterning genes in fins and limbs, we asked whether transcriptional activity of *lmx1bb* in the fin is controlled by similar regulatory logic through *LARM* elements. Previous analysis found that the *LARM*s are conserved among tetrapods as well as the coelacanth, but orthologs could not be found in non-sarcopterygian fishes.[1] In the mouse genome, *LARM* elements occupy an ~6 kb interval located ~60 kb upstream of the *Lmx1b* transcription start site. *Lmx1b* is the only coding gene within a topologically associated domain (TAD) that spans from the 3′ end of the upstream *Mvb12b* gene to the promoter of the downstream *Zbtb43* gene (Figure S3A). We find that this syntenic relationship is maintained across gnathostomes and, to some extent, also preserved in cyclostomes, the lampreys and hagfish (Figure S3B).

To identify putative *LARM* orthologs in species outside of the lobe-finned fish lineage, we generated a hidden Markov model (HMM) using multiple alignments of *LARM* sequences from 12 sarcopterygian species (Table S2). We then used this HMM to search for *LARM* elements in the genomes of species representing major vertebrate lineages. This approach identified *LARM1* and *LARM2* orthologs across jawed vertebrates (Figure 2A) but not cyclostomes. Among gnathostomes, *LARM1s* exhibits the highest sequence conservation and was identified in each species examined, suggesting that *LARM1s* represents a core

Please cite this article in press as: Hawkins et al., The origin and evolution of dorsal determination mechanisms in vertebrate paired appendages, Current Biology (2026), https://doi.org/10.1016/j.cub.2026.05.046



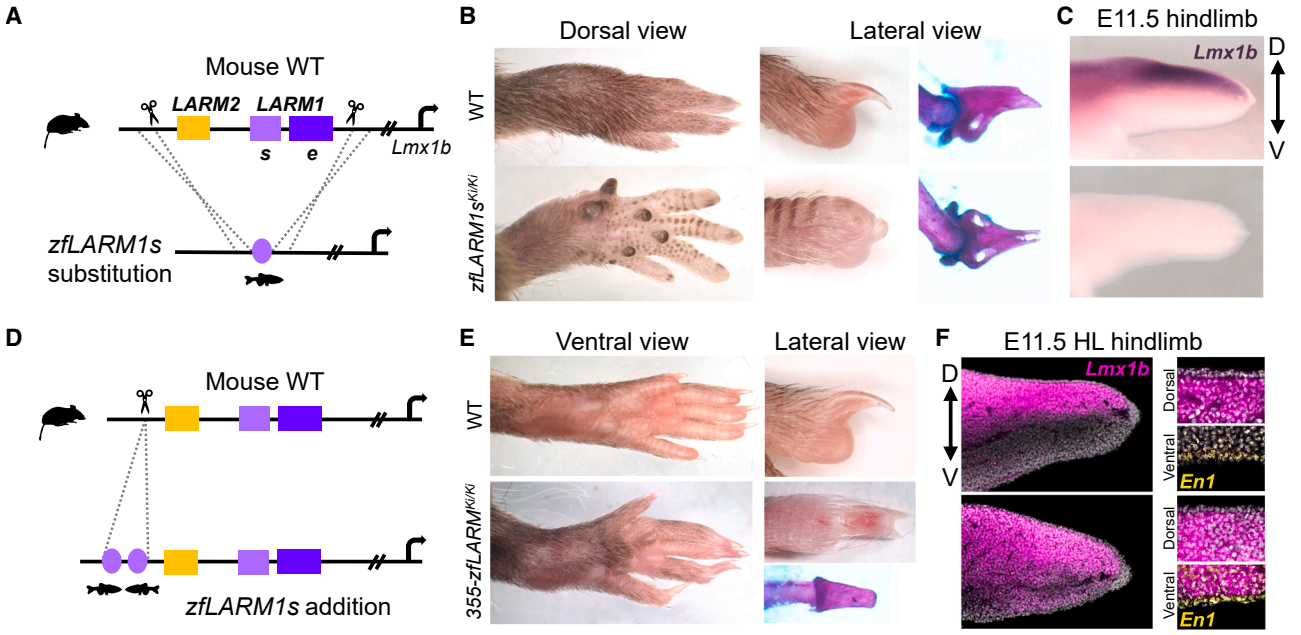


**Figure 3. The zebrafish *LARM1s* element is not sufficient to drive dorsal fates in mice but has additive effects with mouse *LARM***

(A) Transgenic design to test the activity of zebrafish *LARM1s* conserved element (164 bp) in place of the endogenous *LARM* region (7.6 kb) in mouse limb patterning (dotted lines indicate homology arms).

(B and C) (B) Zebrafish *LARM1s* element is not sufficient for the development of dorsal features as *zfLARM1s*$^{Ki/Ki}$ mice have double-ventral limbs and (C) lack *Lmx1b* expression in the dorsal limb mesenchyme.

(D) Schematic of *355-zfLARM* $^{Ki}$ allele in which two *zfLARM1s* elements are incorporated in addition to the endogenous mouse *LARM*s (dotted lines indicate insertion site).

(E and F) (E) The limbs of *355-zfLARM* $^{Ki/Ki}$ mice express a double-dorsal phenotype and (F) display ectopic ventral expression of *Lmx1b*, while *En1* is maintained in the ventral ectoderm. Distal to right; d, dorsal; v, ventral.

See also Figure S5 and Tables S1, S2, and S3.

functional element. In cartilaginous fishes, *LARM1e* was identified in both skate and catshark, but a partial *LARM2* element could be identified only in the catshark. Consistent with previous findings and a more proximate evolutionary distance, *LARM1e* and *LARM2* elements were highly conserved in the non-tetrapod sarcopterygians, the coelacanth and the Australian lungfish. For ray-finned fishes, *LARM1e*, *LARM1s*, and *LARM2* orthologs were identified in the spotted gar, but teleosts exhibited varied conservation of these elements. Although *LARM1s* and a partial (non-significant) *LARM2* sequence were identified in zebrafish, medaka only retains the *LARM1s* element, and *LARM1e* was not detected in either species.

Although not detected by our first HMM, VISTA (visualization tool for alignments) analysis of teleost *mvb12bb-lmx1bb* intergenic regions show a conserved peak just downstream of *LARM1s* in a position analogous to *LARM1e* in tetrapods (Figure S5). Multiple sequence alignment of this region revealed conservation with lobe-finned *LARM1e* elements and the presence of predicted *Lmx1b* transcription factor binding motifs, confirming the identity of this region as the teleost *LARM1e* element (Figure S7). To better characterize *LARM*s in ray-finned fishes and to search for potential *fish versions* of these elements, we generated an additional HMM profile based on ray-finned fish sequences (Table S2). Using a ray-finned fish-derived HMM, we found overlap with *LARM1s* and *LARM1e* hits from the original lobe-finned fish-based HMM, indicating consistency between the two approaches (Table S2). However, the ray-finned fish-based HMM could only detect *LARM2* elements in sarcopterygian genomes up to coelacanth, not in lungfish or tetrapods, suggesting substantial divergence of this element across bony vertebrates. The ray-finned fish-based HMM also failed to identify *LARM* orthologs in cyclostomes. Interestingly, in all teleosts examined, *LARM* elements are only found upstream of the *lmx1bb* paralog and not *lmx1ba*, suggesting that sub-functionalization of DV patterning activity between paralogs occurred following the teleost-specific whole-genome duplication. This is consistent with our finding that loss of *lmx1ba* had no effect on zebrafish fin DV patterning (Figure 1E).

To determine whether non-sarcopterygian *LARM* elements can drive expression in the paired appendages, we used reporter transgene assays in zebrafish using different *LARM* orthologs (Table S2). Using this approach, we found that all *LARM* orthologs tested were sufficient to drive reporter expression in a similar pattern in the developing pectoral fins in transgenic zebrafish, at both the transcript (Figure 2B) and protein levels (Figure S4), demonstrating their functional conservation across gnathostome lineages. Additionally, these results indicate that the *LARM1s* ortholog, an element with a putative silencer function based on mouse and chicken enhancer reporter assays,[1] activates transgene expression in zebrafish (Figure 2B). Local genomic context in which the *LARM* acts may thus impact the effect of these elements on transcription.

Please cite this article in press as: Hawkins et al., The origin and evolution of dorsal determination mechanisms in vertebrate paired appendages, Current Biology (2026), https://doi.org/10.1016/j.cub.2026.05.046



CellPress
OPEN ACCESS

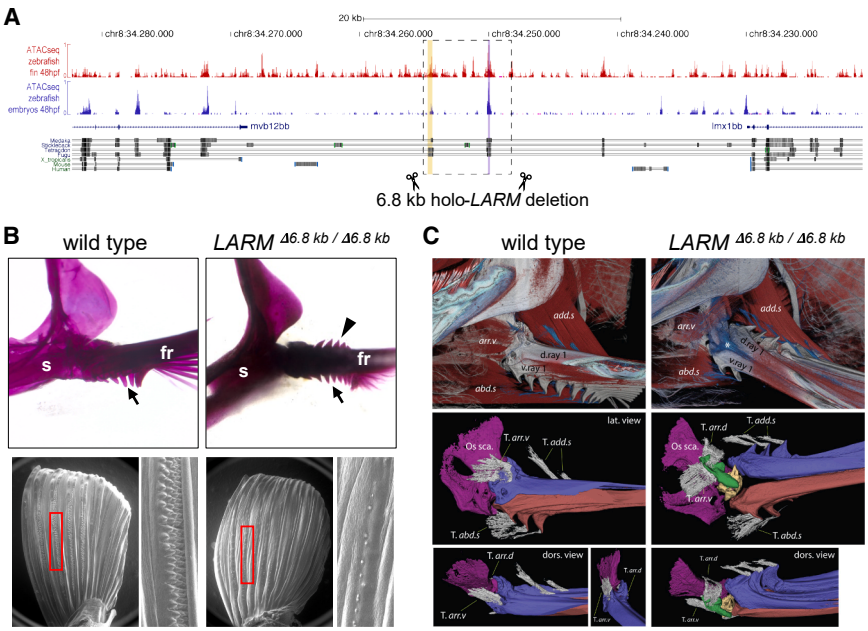


**Figure 4. *LARM*-regulated *Lmx1b*-directed specification of dorsal fate is an ancestral feature of paired appendages**

(A) ATAC-seq profiling reveals open chromatin at the zebrafish *LARM1s* (purple bar) and cryptic *LARM2* (yellow bar) orthologs. The 6.8 kb holo-*LARM* deletion includes both peaks (dashed box). Bottom track indicates sequence conservation (black bars) across bony vertebrate genomes.

(B) $LARM^{\Delta 6.8kb/\Delta 6.8kb}$ mutants develop double-ventral fins with ectopic dorsal flanges (black arrowhead, $n = 10$, 100%). SEM reveals that wild-type males develop tubercle tracts on the pectoral fin dorsal surface (bottom left; $n = 10$; 100%), whereas $LARM^{\Delta 6.8kb/\Delta 6.8kb}$ males do not (bottom right) ($n = 10$, 100%). Red boxes indicate magnified regions.

(C) Transformation of the dorsal hemirays (blue) and musculoskeletal system to the ventral configuration in $LARM^{\Delta 6.8kb/\Delta 6.8kb}$ mutants and the formation of a novel anterior element (green) revealed by immunolabeling ($n = 5$). abd.s, abductor superficialis; add.s, adductor superficialis; arr.d, arrector dorsalis; arr.v, arrector ventralis; d.ray 1, dorsal hemiray 1; Fr, fin rays; Os sca, scapula; v.ray 1, ventral hemiray 1; s, scapulocoracoid; T.*, tendon of.

See also Videos S1 and S2 and Table S1.

## *LARM* function is conserved in the development of fins and limbs

In mouse, the *LARM* elements comprise a limb-specific regulatory hub of *Lmx1b*. Targeted removal of both *LARM1* and *LARM2* recapitulates the double-ventral limb phenotype observed in *Lmx1b*-null mutants, while retaining viability and normal *Lmx1b* function in other expression domains.[1] We asked whether the zebrafish element identified by our initial HMM search, a *LARM1s* ortholog (164 bp), shares similar regulatory function. We used CRISPR-Cas9 to generate stable mutant lines in which this element was removed from the zebrafish genome. Surprisingly, homozygous *LARM1s* deletion mutants exhibited normal pectoral fin DV patterning, suggesting that this element alone is not necessary for paired appendage expression of *lmx1bb* (Figure S5A). Concomitantly, we found that this 164 bp zebrafish element was unable to rescue normal DV patterning and *Lmx1b* expression in the distal limb when it replaced the endogenous *LARM1* and *LARM2* elements in transgenic mice (Figures 3A–3C). However, a consistent partial rescue was observed at the elbow, which no longer exhibits the typical dislocation seen in *ΔLARM1/2* homozygous mutants lacking all *Lmx1b* expression in the limbs (Figure S5B).

While generating the above substitution, we serendipitously created a separate allele in which two copies of the 164 bp zebrafish *LARM1s* element were inserted without removing the endogenous mouse *LARM* locus (Figure 3D). Strikingly, this addition produced a distal double-dorsal phenotype, even in heterozygosity (Figure 3E). The extra regulatory input from the two tandem zebrafish elements caused ectopic *Lmx1b* expression in the distal ventral mesoderm (Figure 3F), without alterations in the normal expression patterns of *En1* or *Wnt7a*. Thus, although the zebrafish *LARM1s* does not fully complement the endogenous mouse *LARM*, the element may act as an enhancer in varied genomic contexts, with dose-dependent effects. In support of this notion, transgenesis assays show that the zebrafish *LARM1s* element contains regulatory information to drive pectoral fin expression (Figure 2B), suggesting that the silencer may originally have arisen as an enhancer or as an element with dual functionality. In transgenesis assays, constructs with two copies of the zebrafish *LARM1s* element in tandem caused increased fin GFP expression over single-copy constructs (Figure S4), further supporting a possible booster function of the element. This function could modulate other nearby enhancers and explain the ventrally expanded *Lmx1b* expression and double-dorsal phenotype observed in *355-zfLARM*$^{Ki/Ki}$ mice.

Extending our analysis of *Lmx1b* regulation in zebrafish, we considered the contribution of putative *LARM2* and *LARM1e* elements identified by VISTA alignments and our ray-finned fish-based HMM. Inspection of the *lmx1bb* regulatory landscape in zebrafish assay for transposase-accessible chromatin using sequencing (ATAC-seq) datasets derived from either whole embryos or fins at 48 hpf revealed several upstream open chromatin peaks (Figure 4A). The most prominent peak corresponds to the *LARM1s* ortholog, while another smaller peak overlaps with the *LARM2* element, suggesting a larger regulatory region. Additionally, VISTA genomic alignments of the *Mvb12b-Lmx1b* intergenic region using the Holostean bridge approach[24] revealed distal sequences with low sequence similarity to the *LARM2* region (Figure S5). Considering this, we overlaid the full ~6 kb mouse *LARM* region onto the zebrafish locus using the 164 bp element as an anchoring point and selected for analysis an ~6 kb region that included the putative *LARM2* region. Remarkably, homozygous deletion of this 6.8 kb holo-*LARM* ($LARM^{\Delta 6.8kb/\Delta 6.8kb}$) interval recapitulated the double-ventral fin phenotype observed in crispant animals while avoiding the lethality observed in

Please cite this article in press as: Hawkins et al., The origin and evolution of dorsal determination mechanisms in vertebrate paired appendages, Current Biology (2026), https://doi.org/10.1016/j.cub.2026.05.046



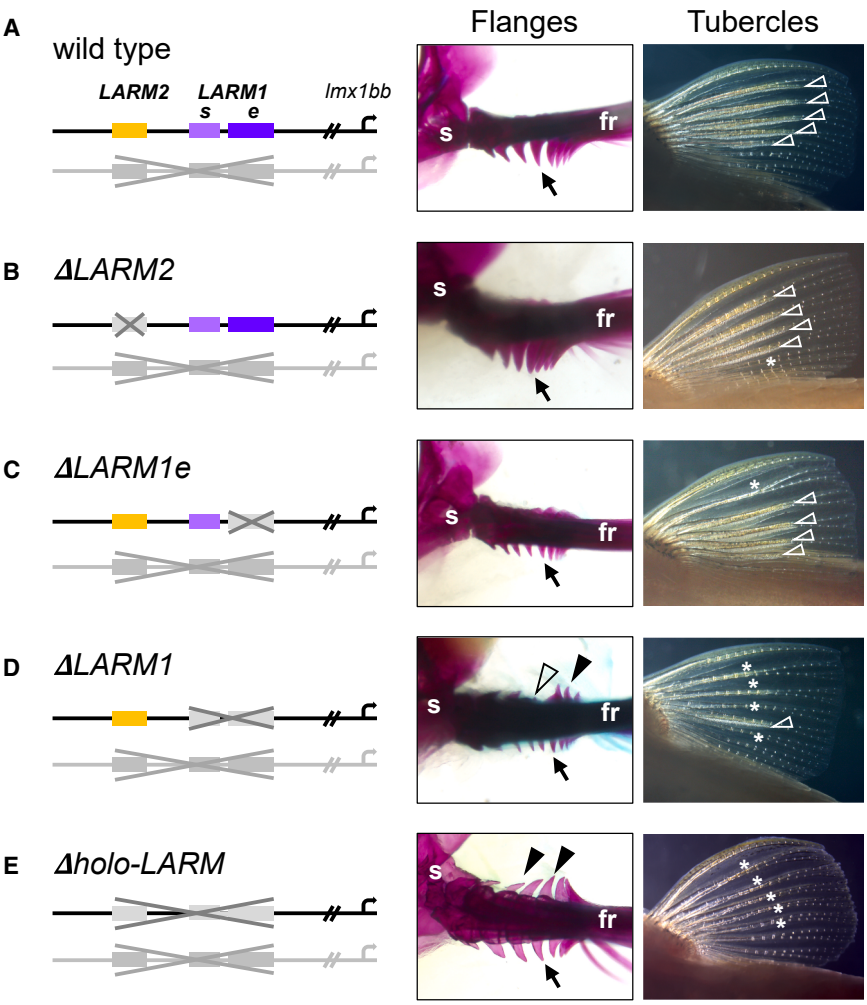


**Figure 5. Deletion of individual *LARM* elements reveals distinct and overlapping functions**

(A–E) Fins from males carrying one holo-*LARM* deletion allele over various individual *LARM* deletions. (A) One wild-type allele is sufficient for normal dorsoventral patterning of ventral flanges (black arrow) and dorsal breeding tubercles on rays 2 through 6 (open white triangles) ($n$ = 20, 100%).

(B) Without *LARM2*, tubercles are absent from ray 6 in roughly half of animals (white asterisk) ($n$ = 21, 62%).

(C) Removal of *LARM1e* results in the occasional absence of breeding tubercles from ray 2 (white asterisk) ($n$ = 20, 10%).

(D) *LARM1* deletion (both *s* and *e* elements) causes incomplete ventralization of the fin rays, where some rays are transformed (black triangle) and others unaffected (open black triangle) ($n$ = 14, 100%). Almost half of animals lack tubercles entirely ($n$ = 14, 43%), and fish that do have tubercles bear them on one or two rays only ($n$ = 8, 57%).

(E) Homozygous $LARM^{\Delta 6.8kb/\Delta 6.8kb}$ mutants exhibit complete ventralization, with dorsal flanges on all fin rays and the absence of dorsal breeding tubercles ($n$ = 20, 100%). fr, fin rays; s, scapulocoracoid.

See also Table S1.

*lmx1bb*-null zebrafish (Figure 4B), phenocopying the removal of *LARM1/2* in the mouse. These results indicate that the zebrafish *LARM* hub retains a conserved regulatory function despite extensive sequence divergence from sarcopterygian orthologs.

The stable $LARM^{\Delta 6.8kb}$ line permitted more thorough anatomical characterization of the double-ventral fin phenotype beyond what was possible with the genetically mosaic *lmx1bb* crispant animals. In addition to dorsal duplication of the bony fin ray flanges, we also observed transformations of the dorsal integument and tendons toward ventral fates. Adult male zebrafish develop tracts of keratinized breeding tubercles on the dorsal surface of the pectoral fin.[25,26] Consistent with a transversion of dorsal to ventral identity of the integument, $LARM^{\Delta 6.8kb/\Delta 6.8kb}$ males failed to develop dorsal tubercle tracts, formed only a few scattered individual tubercles (Figure 4B), and are, accordingly, unsuccessful in mating (Table S3). $LARM^{\Delta 6.8kb/\Delta 6.8kb}$ mutant fins also exhibit shifts in musculoskeletal integration of the dorsal aspect to mirror a ventral configuration (Figure 4C). The dorsal duplication of fin ray flanges was associated with an integrated change in the insertion of the dorsal tendons coming from the adductor superficialis—the primary muscle that elevates and retracts the fin. In wild-type animals, the tendons insert distally on the dorsal surface of the ray, but in the holo-*LARM* deletion animals, the dorsal adductor superficialis tendons instead insert proximally onto the dorsal flanges (Figure 4C). Interestingly, this change did not involve changes to the morphology or integrative capacity of the muscle, suggesting that the dorsal phenotype was restricted to tendon and skeletal tissues (Figure S1).

The most prominent change in $LARM^{\Delta 6.8kb/\Delta 6.8kb}$ fins is the morphology of the anterior first fin ray. In wild-type animals, the dorsal component of the first ray (dorsal hemiray) receives tendinous insertions from two opposite sides of the fin, the arrector dorsalis and arrector ventralis, and articulates with the scapula. Together, this musculoskeletal system acts as a functional unit that controls the leading edge of the fin and moves the first ray dorsally and ventrally. $LARM^{\Delta 6.8kb/\Delta 6.8kb}$ mutants, however, lose this function as the dorsal hemiray does not grow ventrally over the scapula nor does it receive the tendinous attachments of the arrector muscles. These muscles instead attach to a novel bone (Figure 4C, green) located over the anterior side of the scapula (Os sca, purple) and impair proper articulation of the fin. Consequently, $LARM^{\Delta 6.8kb/\Delta 6.8kb}$ mutants are unable to retract the fin to the body as wild-type animals do (Video S1) and swim with their fins extended outward (Video S2). These phenotypic changes in the skeleton, tendons, integument, and articulation match those observed in *LARM* deletion mice and demonstrate that *LARM*-mediated control of *Lmx1b* to specify dorsal appendage fate is a universal feature of paired appendages that arose prior to the origin of limbs.

Please cite this article in press as: Hawkins et al., The origin and evolution of dorsal determination mechanisms in vertebrate paired appendages, Current Biology (2026), https://doi.org/10.1016/j.cub.2026.05.046



CellPress
OPEN ACCESS

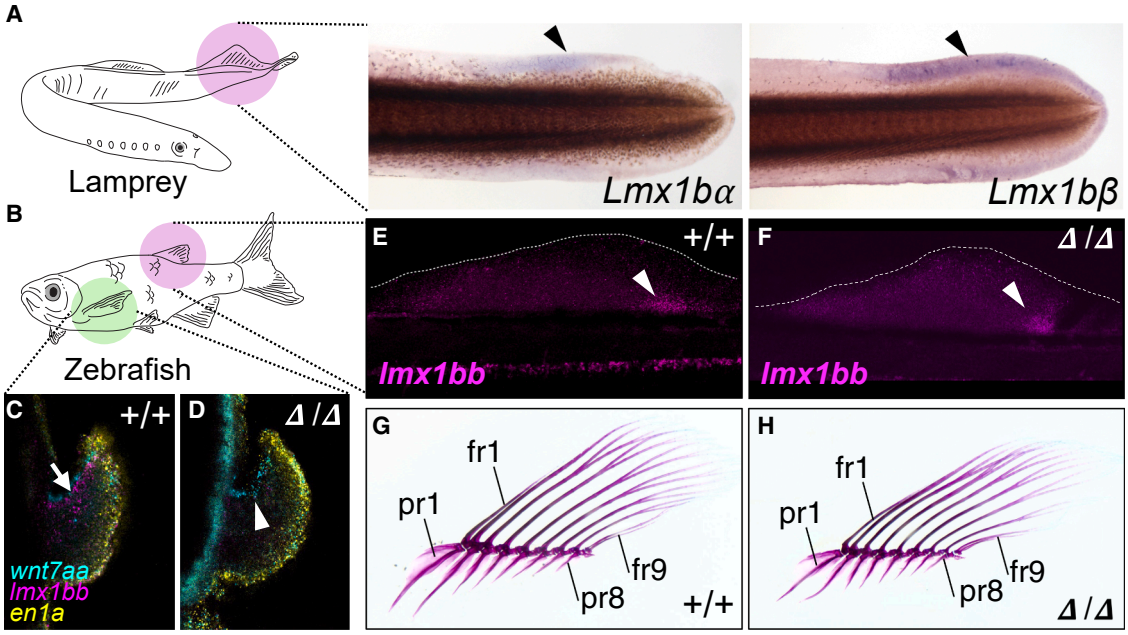


**Figure 6. *Lmx1b* expression in the unpaired fins is an ancient vertebrate feature but does not require *LARM* regulation in gnathostomes**

(A) *Lmx1b* ortholog expression (black arrowheads) in the posterior mesenchyme of the second dorsal fin (purple circle) of lamprey ammocete larvae.

(B) Jawed fishes possess paired fins (green circle) and unpaired midline fins like the dorsal fin (purple circle).

(C) Wild-type zebrafish pectoral fins express *lmx1bb* in the dorsal mesenchyme at 48 hpf (white arrow, $n = 5$).

(D) holo-*LARM* deletion abrogates *lmx1bb* pectoral fin expression (white arrowhead; $n = 5$).

(E) In 14 dpf wild-type fish, *lmx1bb* is expressed in the posterior mesenchyme of the dorsal fin bud (white arrowhead).

(F) Dorsal fin expression is maintained in $LARM^{\Delta 6.8kb/\Delta 6.8kb}$ mutants.

(G) Wild-type adult dorsal fin skeleton with 8 radials and 9 rays ($n = 10$).

(H) $LARM^{\Delta 6.8kb/\Delta 6.8kb}$ mutants exhibit the wild-type dorsal fin pattern ($n = 10$). Dorsal to left, distal to top in (C) and (D); anterior to left, dorsal to top in (A) and (E)—(H). Fr, fin ray; pr, proximal radial.

See also Figure S6; Table S1.

## Individual *LARM* elements have shared, combinatorial functions in fins

In mouse limbs, *Lmx1b* expression in the anterior portion of the autopod is largely controlled by *LARM2*, while *LARM1* drives expression in the posterior domain, and deletion of individual elements results in ventralization of each corresponding region.[1] To investigate the function of individual *LARM*s in the zebrafish, we created stable lines carrying deletions of *LARM1* (removing *s* and *e* regions), *LARM1e*, or *LARM2*. Males from these lines were mated to $LARM^{\Delta 6.8kb/\Delta 6.8kb}$ females so that the phenotypic consequence of individual element deletions could be assessed in the context of deficient *LARM* activity (Figure 5). We find that each individual *LARM* component is necessary for normal regulation of dorsoventral identity, albeit with varied expressivity between elements. Fish without *LARM2* exhibited a propensity to lose the most posterior breeding tubercle tract from the dorsum, but ventralization of the fin ray flanges was not observed (Figure 5B). Removal of *LARM1e* also did not result in fin ray changes but at low frequency caused the loss of the most anterior tubercle tract (Figure 5C). Deletion of the *LARM1* element caused a severe reduction in tubercle formation and frequent but incomplete ventralization of fin rays (Figure 5D). These results demonstrate that all three *LARM* elements are required for normal dorsal patterning of fins.

## *LARM* and the emergence of a paired appendage-specific regulatory program

It is hypothesized that fin patterning programs were first assembled in the midline fins and subsequently co-opted to form the paired appendages later in evolution.[27–31] Recent work has found that *Lmx1b* orthologs are expressed in the posterior mesenchyme of developing dorsal and anal fins of multiple gnathostome lineages, suggesting that this could be an ancestral feature of vertebrate fins that predates the origin of paired appendages.[32] To determine whether median fin *Lmx1b* expression is conserved in cyclostomes—a vertebrate lineage that diverged from gnathostomes prior to the evolution of paired appendages—we assessed the expression of the two *Lmx1b* orthologs in the sea lamprey *Petromyzon marinus*. Embryonic expression of *Lmx1bα* and *Lmx1bβ* in the central nervous system and ear is consistent with conserved roles in gnathostome development (Figure S6A). In the midline fins, we found that both paralogs are expressed in the posterior/caudal domain of the second dorsal fin of advanced ammocoete larvae (Figure 6A), consistent with conservation in gnathostome median fins (Figure 6B).

To determine whether *LARM*-mediated *Lmx1b* regulation is a universal feature of vertebrate appendages or whether *LARM* control is specific to the paired appendage domain, we examined *lmx1bb* expression in $LARM^{\Delta 6.8kb/\Delta 6.8kb}$ zebrafish. Using

Please cite this article in press as: Hawkins et al., The origin and evolution of dorsal determination mechanisms in vertebrate paired appendages, Current Biology (2026), https://doi.org/10.1016/j.cub.2026.05.046



HCR, we found that *lmx1bb* transcripts were lost in mutant pectoral fins at 48 hpf (Figure 6D). However, *lmx1bb* expression domains in other embryonic regions were unaffected (Figure S6B). In the unpaired fins, *lmx1bb* was expressed in the developing dorsal fin buds of zebrafish at 14 days post-fertilization (dpf), with a similar posterior polarity seen in lamprey and jawed fishes[32] (Figure 6E). This shared expression pattern between teleosts and cyclostomes suggests that posteriorly polarized *Lmx1b* expression is an ancestral feature of vertebrate median fins. We asked whether *lmx1bb* expression in the median fins is also *LARM*-mediated, which would be consistent with a universal appendage function with an origin predating the paired appendages. However, in contradiction to the "pan-fin" regulation model, we discovered that dorsal fin *lmx1bb* expression was unaffected in $LARM^{\Delta 6.8kb/\Delta 6.8kb}$ zebrafish (Figure 6F), supporting the paired-appendage-specific nature of *LARM* regulation. The skeletal form of the dorsal fin in the mutants was also unaffected (Figure 6H). These data suggest that, unlike other appendage patterning programs such as nested Hox expression[27] and *Shh* transcription in the ZPA (zone of polarizing activity) controlled by the ZRS (ZPA regulatory sequence),[29] dorsal determination by *LARM*-mediated *Lmx1b* expression likely arose as a novel mechanism in paired appendages, evolving independently from median fin patterning programs specifically within gnathostomes.

### Evolutionary diversification in form and changes in DV regulation

Given the extensive functional anatomical variation observed in the AP and PD axes of fins and limbs across their evolution, it is noteworthy that changes in DV aspects of the appendage skeleton are comparatively constrained. To date, few to no cases of lineage-specific variation in DV polarity of paired appendages have been reported. In a survey of teleost pectoral fin variation, we identified a lineage-specific shift in DV patterning underlying specific adaptive function. Hillstream loaches (families Balitoridae and Gastromyzontidae) have depressed bodies with modified pectoral and pelvic girdles, permitting them to cling to rocks in fast-flowing water and climb waterfalls[33,34] (Figure 7A). Cypriniform fishes outside the hillstream loaches, including non-hillstream loaches such as *Barbatula barbatula* and *Vaillantella maassi*, exhibit a fin configuration similar to that of wild-type zebrafish, in which flanges are found ventrally and there is limited or no elaboration of the fin dorsum (Figures 7B and S7C). Given that a simple fin ray dorsum is found across cypriniform lineages, we infer this to be the ancestral configuration. Strikingly, we discovered that hillstream loaches, nested within the broader loach clade, develop extreme dorsal projections of the proximal fin rays reminiscent of the dorsal flanges we observe in the ventralized fins of holo-*LARM*-deleted zebrafish (Figure 7C). This ventralized condition is derived from the plesiomorphic cypriniform condition of having no dorsal flanges.

Alignment of the *mvb12bb-lmx1bb* intergenic region across cypriniform genomes revealed broad conservation of the *LARM* elements. However, we found a marked reduction in *LARM1e* conservation, specifically within the loach lineage (Figure S7A). Interestingly, this reduction is due in part to lineage-specific deletions in *Beaufortia* species that bear dorsal elaborations (Figure 7D). Deletions in *LARM1e* are compelling candidate changes underlying evolutionary alterations of DV patterning, given that loss of this element caused ventralization in zebrafish fins (Figure 5C). We cloned the *Beaufortia LARM1e* element to verify the deletion and confirmed the same deletion in *Sewellia lineolata*, a species that, together with *Beaufortia*, brackets the ancestral gastromyzontid node,[35] suggesting that the deletion is shared across this family. FIMO (find individual motif occurrences) analysis of the cypriniform *LARM1e* reveals that these deletions in Gastromyzontidae disrupt predicted transcription factor binding sites otherwise conserved across cypriniform fishes (Table S5). Additionally, we find that the *LARM2* element has undergone accelerated sequence evolution in the lineage leading to the hillstream loaches and the family Cobitidae (true loaches) (Figure 7E). This corresponds to dorsal elaborations in true loaches: male loaches develop large dorsal pectoral fin ornaments called *lamina circularis*, which exhibit species-specific morphology[36,37] (Figure 7F). These findings suggest that variations in *LARM* elements have contributed to lineage-specific evolution in teleost paired appendages and may represent a target for adaptive variation of the DV axis.

## DISCUSSION

Of the mechanisms that pattern the three axes of the vertebrate limb, those that specify and pattern the DV axis are the least characterized in terms of developmental genetic programs, evolutionary origins, and natural variation. Our study demonstrates that *Lmx1b* serves as the dorsal determinant in paired fins as well as limbs and that its transcription in the dorsal mesenchyme of both appendage types is controlled by *LARM1* and *LARM2*, which comprise a conserved regulatory hub specifically devoted to the patterning of paired appendages. Results from functional manipulation of the *LARM* elements in zebrafish indicate that conservation of this dorsal program extends to at least the common ancestor of bony vertebrates. The presence of *LARM* orthologs across jawed vertebrates in addition to DV-polarized *Lmx1b* expression in chondrichthyan paired appendages[32,38] suggests that *LARM*-mediated Lmx1b dorsal specification is an ancient feature of paired fins retained from the gnathostome common ancestor. Thus, the dorsal patterning cue was in place prior to the fin-to-limb transition and may have primed limbs to exaggerate DV morphological polarity beyond what is seen in fins, thereby enabling enhanced articulation and integumentary specialization.

Considering this conservation of dorsal determination, we were surprised to find that loss of orthologs of *En1*, which delimits *Lmx1b* activation in the limb, led to ectopic ventral *lmx1bb* expression but had no phenotypic effect on the patterning of the fin. In mouse, while Lmx1b is required for normal dorsal patterning of the zeugopod and autopod limb regions, the effect of En1 in DV patterning is limited to the autopod.[7] A plausible explanation is that zebrafish pectoral fins lack anatomical DV asymmetry at their distal extreme, preventing any ventral-to-dorsal transformation from being detected.

*LARM* regulatory regions are conserved across jawed vertebrates at both the sequence and functional levels, as demonstrated by our zebrafish transgenesis assays. The zebrafish ortholog of the *LARM1s* element exhibited the highest conservation across lineages and was sufficient to drive

Please cite this article in press as: Hawkins et al., The origin and evolution of dorsal determination mechanisms in vertebrate paired appendages, Current Biology (2026), https://doi.org/10.1016/j.cub.2026.05.046



CellPress
OPEN ACCESS

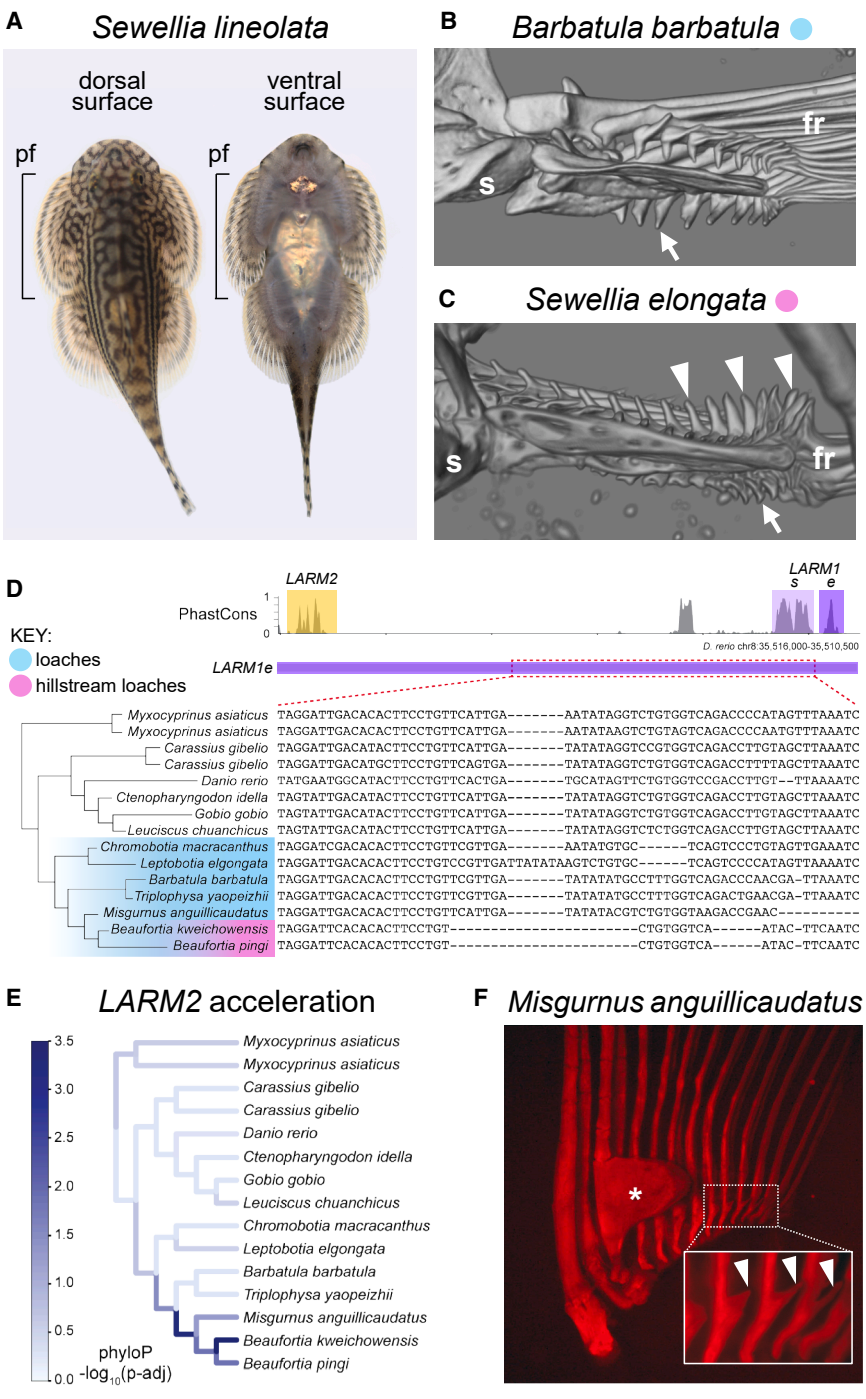


**Figure 7. Lineage-specific evolution of the *LARM* regulatory region in the emergence of novel DV anatomies**

(A) Adult *S. lineolata* hillstream loach.

(B and C) Micro computed-tomography (microCT) reconstructions of the posterior pectoral fin. (B) *B. barbatula*, a non-hillstream loach with distinct ventral flanges (white arrow) and limited dorsal elaboration. (C) The hillstream loach *S. elongata* develops flanges on the dorsal hemitrichia (white arrowheads).

(D) Multiple sequence alignment reveals conservation of *LARM*s across cypriniforms, with lineage-specific *LARM1e* deletions coincident with dorsal ray elaboration.

(E) Cobitid and hillstream loaches exhibit elevated rates of sequence evolution acceleration in the *LARM2* element.

(F) Dorsal pectoral fin ray elaboration in male *M. anguillicaudatus* include the *lamina circularis* (white asterisk) and posterior dorsal flanges (white arrowheads). Anterior to top in (A); proximal to left, distal to top in (B) and (C); anterior to left, distal to top in (F). Fr, fin rays; pf, pectoral fin; s, scapulocoracoid.

See also Figure S7 and Tables S1, S2, S4, and S5.

transgene expression in the fin. Nonetheless, this element was unable to compensate for the loss of endogenous *LARM1* and *LARM2* in transgenic mice, and its removal from the zebrafish genome had no impact on fin DV patterning. However, removal of the 6.8 kb holo-*LARM* region flanking the *LARM1s* core did recapitulate the double-ventral phenotype, indicating that the zebrafish enhancer does contain this regulatory information despite sequence divergence. One interpretation of this result is that the *LARM1s* element serves as a conserved regulatory node or *tent pole*, around which enhancer motifs can appear and disassemble, resulting in lineage-specific sequences and functions with reduced gnathostome-wide conservation outside the *LARM1s* element. Concordantly, genomic alignments between mouse, gar, and zebrafish demonstrate limited conservation at large evolutionary distances (~450 million years), whereas alignment of cypriniform genomes with more proximal divergence times (~175 million years) revealed higher lineage-specific conservation.

For most developmental genetic programs involved in limb axis formation, the prevailing hypothesis is that these patterning mechanisms were first assembled in the midline fins and later co-opted during the origin of paired fins. This framework makes the explicit prediction that paired and midline fins should exhibit similar genetic interactions between patterning molecules and shared regulatory control of gene expression. Indeed, this is the case for *Shh* in the posterior mesenchyme of both paired and midline fins, which is positively regulated by Fgf signaling and is transcriptionally controlled by the ZRS enhancer.[29,31] However, in the case of paired appendage *Lmx1b* regulation we found no such co-optive evolutionary link to median fins. As Zdral et al.[32] recently described, the AP polarity of *Lmx1b* expression in median fins is controlled by Shh signaling, whereas in paired fins *Lmx1b* activation depends on ectodermal Wnt signaling. *LARM*-mediated *Lmx1b* transcriptional control could be an evolutionary innovation that arose

coincident with, or subsequent to, the origin of paired appendages, setting the stage for appendage elaboration in gnathostome lineages.

Although many lineages have elaborated anatomical polarity of the dorsal and ventral regions, evolutionary modification of the DV axis itself is unknown. Unlike the other spatial dimensions of limb and fin structure, variation in the DV axis has not been a source for investigation of clear adaptive variation. Our finding of a distinct phyletic phenocopy[39] in hillstream loaches of the dorsal fin ray flanges provides one such example, paralleling *lmx1bb*-deficient zebrafish. These phenotypic changes correlate with sequence divergence of specific elements of the cypriniform *LARM* hub. These patterns highlight the potential of this locus to facilitate integrated shifts in phenotype and novel function of the fins—in this case adhering to substrates under increased flow conditions.[33,34] Although it is unknown whether these changes at the *LARM* hub were drivers of this change, it is clear that regulatory changes at this locus could initiate or stabilize such morphologies. As we observed in the 6.8 kb holo-*LARM* deletion fins, skeletal changes would be integrated with the musculature and facilitate novel articulation. Importantly, this shift in regulation would provide a robust developmental signal, given the autoregulatory feedback observed at the *LARM*. This would facilitate evolutionary changes in the DV axis of appendage structure and facilitate natural variation within these lineages.

## RESOURCE AVAILABILITY

### Lead contact

Further information and requests for resources and reagents should be directed to and will be fulfilled by the lead contact, Matthew P. Harris (harris@genetics.med.harvard.edu).

### Materials availability

Zebrafish lines generated by the authors will be distributed to other researchers upon request. Sperm from these lines have been deposited with Cryogenetics (www.cryogenetics.com).

### Data and code availability

- Original source data and code for figures in the paper are available and archived at 10.7910/DVN/J3YUZO
- This paper does not report original code.
- Any additional information required to reanalyze the data reported in this paper is available from the lead contact upon request.

## ACKNOWLEDGMENTS

The authors thank Yan Gong for assistance with SEM imaging, Stephen Treaster for curation of cypriniform genomic data, and Laura Galán for characterizing the CRISPR-edited mouse models. Funding for US-based efforts was provided in part by the National Institutes of Health (grant nos. R01HD112906-01 [M.P.H.], R35GM146467 [S.K.M.], and R35GM150590 [J.M.D.]), the National Science Foundation (grant nos. CAREER 1845513 [S.K.M.], OPP 2324998 [J.M.D.], and IOS 2054340 [D.M.M.]). The Spanish Ministry of Science and Innovation provided support for Ros and Tena groups (grant nos. PID2023-147771NB-I00 [M.A.R.] and PID2022-141288NB-I00 [J.J.T.]), while the Scientific Grant Agency of the Slovak Republic grant VEGA 1/0299/26 supported D.J.. The Transgenic Facility, directed by M.S.-M., is supported by the Instituto de Salud Carlos III (ISCIII), co-funded by European Union grant PT23/00123 Intercambios Científicos Lifehub Jump-Start exchange program (M.A.R., J.J.T., and S.Z.).

## AUTHOR CONTRIBUTIONS

Conceptualization, M.B.H., S.Z., M.P.H., J.J.T., and M.A.R.; methodology, all authors; investigation, all authors; writing—original draft, M.B.H., S.Z., M.P.H., J.J.T., and M.A.R.; writing—review & editing, M.B.H., S.Z., M.P.H., J.J.T., and M.A.R.; funding acquisition, D.J., D.M.M., M.P.H., S.K.M., J.J.T., M.A.R., and J.M.D.; resources, M.P.H., J.J.T., and M.A.R.; supervision, M.P.H., J.J.T., and M.A.R.

## DECLARATION OF INTERESTS

The authors declare that they have no competing interests.

## STAR★METHODS

Detailed methods are provided in the online version of this paper and include the following:

- KEY RESOURCES TABLE
- EXPERIMENTAL MODEL AND STUDY PARTICIPANT DETAILS
  - Mouse husbandry
  - Fish husbandry
- METHOD DETAILS
  - Hybridization chain reaction
  - Allele generation in zebrafish with CRISPR-Cas9
  - Mouse strains
  - Skeletal staining
  - Analysis of Hi-C data
  - Identification of *LARM* ortholog sequences in fishes
  - Enhancer reporter assays in zebrafish
  - Whole-mount colorimetric *in situ* hybridization
  - Immunolabelling of pectoral fin musculoskeletal elements
  - Micro computed tomography (μCT)
  - VISTA genome alignments
  - 3D Reconstruction of cypriniform pectoral fin skeletons
  - Loach material and analysis of *LARM1e* element in hillstream loaches
  - SEM imaging of fin tubercles
  - Spawning performance trials
  - Evolutionary rate analysis of cypriniform *LARM* elements
- QUANTIFICATION AND STATISTICAL ANALYSIS

## SUPPLEMENTAL INFORMATION

Supplemental information can be found online at https://doi.org/10.1016/j.cub.2026.05.046.

Received: October 17, 2025
Revised: March 30, 2026
Accepted: May 22, 2026

## REFERENCES

1. Haro, E., Petit, F., Pira, C.U., Spady, C.D., Lucas-Toca, S., Yorozuya, L.I., Gray, A.L., Escande, F., Jourdain, A.-S., Nguyen, A., et al. (2021). Identification of limb-specific Lmx1b auto-regulatory modules with Nail-patella syndrome pathogenicity. Nat. Commun. *12*, 5533. https://doi.org/10.1038/s41467-021-25844-5.
2. Stewart, T.A., Lemberg, J.B., Taft, N.K., Yoo, I., Daeschler, E.B., and Shubin, N.H. (2019). Fin ray patterns at the fin-to-limb transition. Proc. Natl. Acad. Sci. USA *117*, 1612–1620. https://doi.org/10.1073/pnas.1915983117.
3. Parr, B.A., and McMahon, A.P. (1995). Dorsalizing signal Wnt-7a required for normal polarity of D-V and A-P axes of mouse limb. Nature *374*, 350–353. https://doi.org/10.1038/374350a0.

4. Riddle, R.D., Ensini, M., Nelson, C., Tsuchida, T., Jessell, T.M., and Tabin, C. (1995). Induction of the LIM Homeobox Gene Lmx1 by WNT6a Establishes Dorsoventral Pattern in the Vertebrate Limb. Cell *83*, 631–640. https://doi.org/10.1016/0092-8674(95)90103-5.

5. Vogel, A., Rodriguez, C., Warnken, W., and Belmonte, J.C.I. (1995). Dorsal cell fate specified by chick Lmxl during vertebrate limb development. Nature *378*, 716–720. https://doi.org/10.1038/378716a0.

6. Yang, Y., and Niswander, L. (1995). Interaction between the signaling molecules WNT7a and SHH during vertebrate limb development: dorsal signals regulate anteroposterior patterning. Cell *80*, 939–947. https://doi.org/10.1016/0092-8674(95)90297-x.

7. Loomis, C.A., Harris, E., Michaud, J., Wurst, W., Hanks, M., and Joyner, A.L. (1996). The mouse Engrailed-1 gene and ventral limb patterning. Nature *382*, 360–363. https://doi.org/10.1038/382360a0.

8. Chen, H., Lun, Y., Ovchinnikov, D., Kokubo, H., Oberg, K.C., Pepicelli, C.V., Can, L., Lee, B., and Johnson, R.L. (1998). Limb and kidney defects in Lmx1b mutant mice suggest an involvement of LMX1B in human nail patella syndrome. Nat. Genet. *19*, 51–55. https://doi.org/10.1038/ng0598-51.

9. Chen, H., Ovchinnikov, D., Pressman, C.L., Aulehla, A., Lun, Y., and Johnson, R.L. (1998). Multiple calvarial defects in lmx1b mutant mice. Dev. Genet. *22*, 314–320. https://doi.org/10.1002/(SICI)1520-6408(1998)22:4<314::AID-DVG2>3.0.CO;2-9.

10. Logan, C., Hornbruch, A., Campbell, I., and Lumsden, A. (1997). The role of Engrailed in establishing the dorsoventral axis of the chick limb. Development *124*, 2317–2324. https://doi.org/10.1242/dev.124.12.2317.

11. Haro, E., Watson, B.A., Feenstra, J.M., Tegeler, L., Pira, C.U., Mohan, S., and Oberg, K.C. (2017). Lmx1b-targeted cis-regulatory modules involved in limb dorsalization. Development *144*, 2009–2020. https://doi.org/10.1242/dev.146332.

12. Dealy, C.N., Roth, A., Ferrari, D., Brown, A.M.C., and Kosher, R.A. (1993). Wnt-5a and Wnt-7a are expressed in the developing chick limb bud in a manner suggesting roles in pattern formation along the proximodistal and dorsoventral axes. Mech. Dev. *43*, 175–186. https://doi.org/10.1016/0925-4773(93)90034-u.

13. Ekker, M., Wegner, J., Andrée Akimenko, M.A., and Westerfield, M. (1992). Coordinate embryonic expression of three zebrafish engrailed genes. Development *116*, 1001–1010. https://doi.org/10.1242/dev.116.4.1001.

14. Reifers, F., Böhli, H., Walsh, E.C., Crossley, P.H., Stainier, D.Y.R., and Brand, M. (1998). Fgf8 is mutated in zebrafish acerebellar (ace) mutants and is required for maintenance of midbrain-hindbrain boundary development and somitogenesisy. Development *125*, 2381–2395. https://doi.org/10.1242/dev.125.13.2381.

15. Neumann, C.J., Grandel, H., Gaffield, W., Schulte-Merker, S., and Nüsslein-Volhard, C. (1999). Transient establishment of anteroposterior polarity in the zebrafish pectoral fin bud in the absence of sonic hedgehog activity. Development *126*, 4817–4826. https://doi.org/10.1242/dev.126.21.4817.

16. Grandel, H., Draper, B.W., and Schulte-Merker, S. (2000). dackel acts in the ectoderm of the zebrafish pectoral fin bud to maintain AER signaling. Development *127*, 4169–4178. https://doi.org/10.1242/dev.127.19.4169.

17. Uemura, O., Okada, Y., Ando, H., Guedj, M., Higashijima, S.-I., Shimazaki, T., Chino, N., Okano, H., and Okamoto, H. (2005). Comparative functional genomics revealed conservation and diversification of three enhancers of the isl1 gene for motor and sensory neuron-specific expression. Dev. Biol. *278*, 587–606. https://doi.org/10.1016/j.ydbio.2004.11.031.

18. Schweizer, H., Johnson, R.L., and Brand-Saberi, B. (2004). Characterization of migration behavior of myogenic precursor cells in the limb bud with respect to Lmx1b expression. Anat. Embryol. *208*, 7–18. https://doi.org/10.1007/s00429-003-0373-y.

19. Jagla, K., Dollé, P., Mattei, M.G., Jagla, T., Schuhbaur, B., Dretzen, G., Bellard, F., and Bellard, M. (1995). Mouse Lbx1 and human LBX1 define a novel mammalian homeobox gene family related to the Drosophila lady bird genes. Mech. Dev. *53*, 345–356. https://doi.org/10.1016/0925-4773(95)00450-5.

20. Seger, C., Hargrave, M., Wang, X., Chai, R.J., Elworthy, S., and Ingham, P.W. (2011). Analysis of Pax7 expressing myogenic cells in zebrafish muscle development, injury, and models of disease. Dev. Dyn. *240*, 2440–2451. https://doi.org/10.1002/dvdy.22745.

21. Minchin, J.E.N., Williams, V.C., Hinits, Y., Low, S., Tandon, P., Fan, C.-M., Rawls, J.F., and Hughes, S.M. (2013). Oesophageal and sternohyal muscle fibres are novel Pax3-dependent migratory somite derivatives essential for ingestion. Development *140*, 2972–2984. https://doi.org/10.1242/dev.090050.

22. Burzynski, G.M., Reed, X., Maragh, S., Matsui, T., and McCallion, A.S. (2013). Integration of genomic and functional approaches reveals enhancers at LMX1A and LMX1B. Mol. Genet. Genomics *288*, 579–589. https://doi.org/10.1007/s00438-013-0771-7.

23. Schibler, A., and Malicki, J. (2007). A screen for genetic defects of the zebrafish ear. Mech. Dev. *124*, 592–604. https://doi.org/10.1016/j.mod.2007.04.005.

24. Braasch, I., Gehrke, A.R., Smith, J.J., Kawasaki, K., Manousaki, T., Pasquier, J., Amores, A., Desvignes, T., Batzel, P., Catchen, J., et al. (2016). The spotted gar genome illuminates vertebrate evolution and facilitates human-teleost comparisons. Nat. Genet. *48*, 427–437. https://doi.org/10.1038/ng.3526.

25. Kang, J., Nachtrab, G., and Poss, K.D. (2013). Local Dkk1 crosstalk from breeding ornaments impedes regeneration of injured male zebrafish fins. Dev. Cell *27*, 19–31. https://doi.org/10.1016/j.devcel.2013.08.015.

26. McMillan, S.C., Xu, Z.T., Zhang, J., Teh, C., Korzh, V., Trudeau, V.L., and Akimenko, M.-A. (2013). Regeneration of breeding tubercles on zebrafish pectoral fins requires androgens and two waves of revascularization. Development *140*, 4323–4334. https://doi.org/10.1242/dev.095992.

27. Freitas, R., Zhang, G., and Cohn, M.J. (2006). Evidence that mechanisms of fin development evolved in the midline of early vertebrates. Nature *442*, 1033–1037. https://doi.org/10.1038/nature04984.

28. Dahn, R.D., Davis, M.C., Pappano, W.N., and Shubin, N.H. (2007). Sonic hedgehog function in chondrichthyan fins and the evolution of appendage patterning. Nature *445*, 311–314. https://doi.org/10.1038/nature05436.

29. Letelier, J., de la Calle-Mustienes, E., Pieretti, J., Naranjo, S., Maeso, I., Nakamura, T., Pascual-Anaya, J., Shubin, N.H., Schneider, I., Martinez-Morales, J.R., et al. (2018). A conserved Shh cis-regulatory module highlights a common developmental origin of unpaired and paired fins. Nat. Genet. *50*, 504–509. https://doi.org/10.1038/s41588-018-0080-5.

30. Letelier, J., Naranjo, S., Sospedra-Arrufat, I., Martínez-Morales, J.R., López-Ríos, J., Shubin, N., and Gómez-Skarmeta, J.L. (2021). The Shh/Gli3 gene regulatory network precedes the origin of paired fins and reveals the deep homology between distal fins and digits. Proc. Natl. Acad. Sci. USA *118*. https://doi.org/10.1073/pnas.2100575118.

31. Hawkins, M.B., Jandzik, D., Tulenko, F.J., Cass, A.N., Nakamura, T., Shubin, N.H., Davis, M.C., and Stock, D.W. (2022). An Fgf-Shh positive feedback loop drives growth in developing unpaired fins. Proc. Natl. Acad. Sci. USA *119*, e2120150119. https://doi.org/10.1073/pnas.2120150119.

32. Zdral, S., Bordignon, S.G., Meyer, A., Ros, M.A., and Woltering, J.M. (2026). Dorsoventral limb patterning in paired appendages emerged via regulatory repurposing of an ancestral posterior fin module. Mol. Biol. Evol. *43*, msaf331. https://doi.org/10.1093/molbev/msaf331.

33. Willis, J., Burt de Perera, T., Newport, C., Poncelet, G., Sturrock, C.J., and Thomas, A. (2019). The structure and function of the sucker systems of hill stream loaches. Preprint at bioRxiv. https://doi.org/10.1101/851592.

34. Crawford, C.H., Randall, Z.S., Hart, P.B., Page, L.M., Chakrabarty, P., Suvarnaraksha, A., and Flammang, B.E. (2020). Skeletal and muscular pelvic morphology of hillstream loaches (Cypriniformes: Balitoridae). J. Morphol. *281*, 1280–1295. https://doi.org/10.1002/jmor.21247.

35. Chen, X.J., Song, L., and Liu, W.Z. (2022). Seven fish complete mitochondrial genomes of the Gastromyzontidae in Southern China (Teleostei: Cypriniformes). Mitochondrial DNA B *7*, 624–626. https://doi.org/10.1080/23802359.2022.2055983.

36. Havird, J.C., and Page, L.M. (2010). A revision of Lepidocephalichthys (teleostei: Cobitidae) with descriptions of two new species from Thailand, Laos, Vietnam, and Myanmar. Copeia *2010*, 137–159. https://doi.org/10.1643/ci-08-240.

37. Yashima, Y., Okada, R., and Kitagawa, T. (2023). Differences in sexual morphological dimorphisms between two loach species of the genus Misgurnus (Cypriniformes: Cobitidae) in the River Shono system, Fukui Prefecture, Japan. J. Vertebr. Biol. *72*. 23035.1-14. https://doi.org/10.25225/jvb.23035.

38. Jung, H., Baek, M., D'Elia, K.P., Boisvert, C., Currie, P.D., Tay, B.-H., Venkatesh, B., Brown, S.M., Heguy, A., Schoppik, D., et al. (2018). The ancient origins of neural substrates for land walking. Cell *172*, 667–682. https://doi.org/10.1016/j.cell.2018.01.013.

39. Stebbins, G.L., and Basile, D.V. (1986). Phyletic phenocopies: A useful technique for probing the genetic and developmental basis of evolutionary change. Evolution *40*, 422–425. https://doi.org/10.1111/j.1558-5646.1986.tb00483.x.

40. Montague, T.G., Cruz, J.M., Gagnon, J.A., Church, G.M., and Valen, E. (2014). CHOPCHOP: a CRISPR/Cas9 and TALEN web tool for genome editing. Nucleic Acids Res. *42*, W401–W407. https://doi.org/10.1093/nar/gku410.

41. Siepel, A., Bejerano, G., Pedersen, J.S., Hinrichs, A.S., Hou, M., Rosenbloom, K., Clawson, H., Spieth, J., Hillier, L.W., Richards, S., et al. (2005). Evolutionarily conserved elements in vertebrate, insect, worm, and yeast genomes. Genome Res. *15*, 1034–1050. https://doi.org/10.1101/gr.3715005.

42. Hubisz, M.J., Pollard, K.S., and Siepel, A. (2011). PHAST and RPHAST: phylogenetic analysis with space/time models. Brief. Bioinform. *12*, 41–51. https://doi.org/10.1093/bib/bbq072.

43. R Development Core Team (2008). R: a Language and Environment for Statistical Computing (R Foundation for Statistical Computing). https://www.r-project.org/.

44. Perez, G., Barber, G.P., Benet-Pages, A., Casper, J., Clawson, H., Diekhans, M., Fischer, C., Gonzalez, J.N., Hinrichs, A.S., Lee, C.M., et al. (2025). The UCSC Genome Browser database: 2025 update. Nucleic Acids Res. *53*, D1243–D1249. https://doi.org/10.1093/nar/gkae974.

45. Waterhouse, A.M., Procter, J.B., Martin, D.M.A., Clamp, M., and Barton, G.J. (2009). Jalview version 2—a multiple sequence alignment editor and analysis workbench. Bioinformatics *25*, 1189–1191. https://doi.org/10.1093/bioinformatics/btp033.

46. Dubchak, I., Brudno, M., Loots, G.G., Pachter, L., Mayor, C., Rubin, E.M., and Frazer, K.A. (2000). Active conservation of noncoding sequences revealed by three-way species comparisons. Genome Res. *10*, 1304–1306. https://doi.org/10.1101/gr.142200.

47. Frazer, K.A., Pachter, L., Poliakov, A., Rubin, E.M., and Dubchak, I. (2004). VISTA: computational tools for comparative genomics. Nucleic Acids Res. *32*, W273–W279. https://doi.org/10.1093/nar/gkh458.

48. Armstrong, J., Hickey, G., Diekhans, M., Fiddes, I.T., Novak, A.M., Deran, A., Fang, Q., Xie, D., Feng, S., Stiller, J., et al. (2020). Progressive Cactus is a multiple-genome aligner for the thousand-genome era. Nature *587*, 246–251. https://doi.org/10.1038/s41586-020-2871-y.

49. Sandelin, A., Alkema, W., Engström, P., Wasserman, W.W., and Lenhard, B. (2004). JASPAR: an open-access database for eukaryotic transcription factor binding profiles. Nucleic Acids Res. *32*, 91D–994. https://doi.org/10.1093/nar/gkh012.

50. Aleström, P., D'Angelo, L., Midtlyng, P.J., Schorderet, D.F., Schulte-Merker, S., Sohm, F., and Warner, S. (2020). Zebrafish: Housing and husbandry recommendations. Lab. Anim. *54*, 213–224. https://doi.org/10.1177/0023677219869037.

51. Kimmel, C.B., Ballard, W.W., Kimmel, S.R., Ullmann, B., and Schilling, T.F. (1995). Stages of embryonic development of the zebrafish. Dev. Dyn. *203*, 253–310. https://doi.org/10.1002/aja.1002030302.

52. Choi, H.M.T., Calvert, C.R., Husain, N., Huss, D., Barsi, J.C., Deverman, B.E., Hunter, R.C., Kato, M., Lee, S.M., Abelin, A.C.T., et al. (2016). Mapping a multiplexed zoo of mRNA expression. Development *143*, 3632–3637. https://doi.org/10.1242/dev.140137.

53. Elagoz, A.M., Styfhals, R., Maccuro, S., Masin, L., Moons, L., and Seuntjens, E. (2022). Optimization of whole mount RNA multiplexed in situ hybridization chain reaction with immunohistochemistry, clearing and imaging to visualize octopus embryonic neurogenesis. Front. Physiol. *13*, 882413. https://doi.org/10.3389/fphys.2022.882413.

54. Morabito, A., Malkmus, J., Pancho, A., Zuniga, A., Zeller, R., and Sheth, R. (2023). Optimized protocol for whole-mount RNA fluorescent in situ hybridization using oxidation-mediated autofluorescence reduction on mouse embryos. Star Protoc. *4*, 102603. https://doi.org/10.1016/j.xpro.2023.102603.

55. Labun, K., Montague, T.G., Gagnon, J.A., Thyme, S.B., and Valen, E. (2016). CHOPCHOP v2: a web tool for the next generation of CRISPR genome engineering. Nucleic Acids Res. *44*, W272–W276. https://doi.org/10.1093/nar/gkw398.

56. Sentmanat, M.F., Peters, S.T., Florian, C.P., Connelly, J.P., and Pruett-Miller, S.M. (2018). A survey of validation strategies for CRISPR-Cas9 editing. Sci. Rep. *8*, 888. https://doi.org/10.1038/s41598-018-19441-8.

57. Labun, K., Montague, T.G., Krause, M., Torres Cleuren, Y.N., Tjeldnes, H., and Valen, E. (2019). CHOPCHOP v3: expanding the CRISPR web toolbox beyond genome editing. Nucleic Acids Res. *47*, W171–W174. https://doi.org/10.1093/nar/gkz365.

58. Marlétaz, F., de la Calle-Mustienes, E., Acemel, R.D., Paliou, C., Naranjo, S., Martínez-García, P.M., Cases, I., Sleight, V.A., Hirschberger, C., Marcet-Houben, M., et al. (2023). The little skate genome and the evolutionary emergence of wing-like fins. Nature *616*, 495–503. https://doi.org/10.1038/s41586-023-05868-1.

59. Franke, M., De la Calle-Mustienes, E., Neto, A., Almuedo-Castillo, M., Irastorza-Azcarate, I., Acemel, R.D., Tena, J.J., Santos-Pereira, J.M., and Gómez-Skarmeta, J.L. (2021). CTCF knockout in zebrafish induces alterations in regulatory landscapes and developmental gene expression. Nat. Commun. *12*, 1–19. https://doi.org/10.1038/s41467-021-25604-5.

60. Kraft, K., Magg, A., Heinrich, V., Riemenschneider, C., Schöpflin, R., Markowski, J., Ibrahim, D.M., Acuna-Hidalgo, R., Despang, A., Andrey, G., et al. (2019). Serial genomic inversions induce tissue-specific architectural stripes, gene misexpression and congenital malformations. Nat. Cell Biol. *21*, 305–310. https://doi.org/10.1038/s41556-019-0273-x.

61. Wheeler, T.J., and Eddy, S.R. (2013). nhmmer: DNA homology search with profile HMMs. Bioinformatics *29*, 2487–2489. https://doi.org/10.1093/bioinformatics/btt403.

62. Larkin, M.A., Blackshields, G., Brown, N.P., Chenna, R., McGettigan, P.A., McWilliam, H., Valentin, F., Wallace, I.M., Wilm, A., Lopez, R., et al. (2007). Clustal W and Clustal X version 2.0. Bioinformatics *23*, 2947–2948. https://doi.org/10.1093/bioinformatics/btm404.

63. Kawakami, K. (2007). Tol2: a versatile gene transfer vector in vertebrates. Genome Biol. *8*, S7. https://doi.org/10.1186/gb-2007-8-s1-s7.

64. Kawakami, K., Takeda, H., Kawakami, N., Kobayashi, M., Matsuda, N., and Mishina, M. (2004). A transposon-mediated gene trap approach identifies developmentally regulated genes in zebrafish. Dev. Cell *7*, 133–144. https://doi.org/10.1016/j.devcel.2004.06.005.

65. Gehrke, A.R., Schneider, I., de la Calle-Mustienes, E., Tena, J.J., Gomez-Marin, C., Chandran, M., Nakamura, T., Braasch, I., Postlethwait, J.H., Gómez-Skarmeta, J.L., et al. (2015). Deep conservation of wrist and digit enhancers in fish. Proc. Natl. Acad. Sci. USA *112*, 803–808. https://doi.org/10.1073/pnas.1420208112.

66. Jowett, T., and Lettice, L. (1994). Whole-mount in situ hybridizationon zebrafish embryos using a mixture of digoxigenin- and fluorescein-labelled probes. Trends Genet. *10*, 73–74. https://doi.org/10.1016/0168-9525(94)90220-8.

67. Lufkin, T. (2007). In situ hybridization of whole-mount mouse embryos with RNA probes: hybridization, washes, and histochemistry. Cold Spring Harb. Protoc. *2007*, pdb.prot4823. https://doi.org/10.1101/pdb.prot4823.

68. Cattell, M., Lai, S., Cerny, R., and Medeiros, D.M. (2011). A new mechanistic scenario for the origin and evolution of vertebrate cartilage. PLoS One *6*, e22474. https://doi.org/10.1371/journal.pone.0022474.

69. Tahara, Y. (1988). Normal stages of development in the lamprey, Lampetra reissued (dybowski). Zool. Sci. *5*, 109–118.

70. Meulemans, D., and Bronner-Fraser, M. (2002). Amphioxus and lamprey AP-2 genes: implications for neural crest evolution and migration patterns. Development *129*, 4953–4962. https://doi.org/10.1242/dev.129.21.4953.

71. Pende, M., Vadiwala, K., Schmidbaur, H., Stockinger, A.W., Murawala, P., Saghafi, S., Dekens, M.P.S., Becker, K., Revilla-i-Domingo, R., Papadopoulos, S.C., et al. (2020). A versatile depigmentation, clearing, and labeling method for exploring nervous system diversity. Sci. Adv. *6*, eaba0365. https://doi.org/10.1126/sciadv.aba0365.

72. Brudno, M., Do, C.B., Cooper, G.M., Kim, M.F., Davydov, E., NISC; Comparative; Sequencing Program, Green, E.D., Sidow, A., and Batzoglou, S. (2003). LAGAN and Multi-LAGAN: efficient tools for large-scale multiple alignment of genomic DNA. Genome Res. *13*, 721–731. https://doi.org/10.1101/gr.926603.

73. Blackburn, D.C., Boyer, D.M., Gray, J.A., Winchester, J., Bates, J.M., Baumgart, S.L., Braker, E., Coldren, D., Conway, K.W., Rabosky, A.D., et al. (2024). Increasing the impact of vertebrate scientific collections through 3D imaging: The openVertebrate (oVert) Thematic Collections Network. BioScience *74*, 169–186. https://doi.org/10.1093/biosci/biad120.

74. Schindelin, J., Rueden, C.T., Hiner, M.C., and Eliceiri, K.W. (2015). The ImageJ ecosystem: An open platform for biomedical image analysis. Mol. Reprod. Dev. *82*, 518–529. https://doi.org/10.1002/mrd.22489.

75. Camacho, C., Coulouris, G., Avagyan, V., Ma, N., Papadopoulos, J., Bealer, K., and Madden, T.L. (2009). BLAST+: architecture and applications. BMC Bioinform. *10*, 421. https://doi.org/10.1186/1471-2105-10-421.

76. Stout, C.C., Tan, M., Lemmon, A.R., Lemmon, E.M., and Armbruster, J.W. (2016). Resolving Cypriniformes relationships using an anchored enrichment approach. BMC Evol. Biol. *16*, 244. https://doi.org/10.1186/s12862-016-0819-5.

77. Wang, Y., Shen, Y., Feng, C., Zhao, K., Song, Z., Zhang, Y., Yang, L., and He, S. (2016). Mitogenomic perspectives on the origin of Tibetan loaches and their adaptation to high altitude. Sci. Rep. *6*, 29690. https://doi.org/10.1038/srep29690.

78. Pollard, K.S., Hubisz, M.J., Rosenbloom, K.R., and Siepel, A. (2010). Detection of nonneutral substitution rates on mammalian phylogenies. Genome Res. *20*, 110–121. https://doi.org/10.1101/gr.097857.109.

79. Grant, C.E., Bailey, T.L., and Noble, W.S. (2011). FIMO: scanning for occurrences of a given motif. Bioinformatics *27*, 1017–1018. https://doi.org/10.1093/bioinformatics/btr064.

Please cite this article in press as: Hawkins et al., The origin and evolution of dorsal determination mechanisms in vertebrate paired appendages, Current Biology (2026), https://doi.org/10.1016/j.cub.2026.05.046



## STAR★METHODS

### KEY RESOURCES TABLE

| REAGENT or RESOURCE | SOURCE | IDENTIFIER |
|---|---|---|
| **Deposited data** | | |
| Original source data and code for figures in the paper are available and archived at https://doi.org/10.7910/DVN/J3YUZO | | |
| **Experimental models: Organisms/strains** | | |
| Mouse: Lmx1bDelLARM1/2;ZFLARMemMaros Genetic description The mouse Lmx1b enhancers LARM 1 and 2 (aprox 7Kb deletion) were substituted by the ortholog zebrafish LARM enhancer (164bp) Current genetic background C57BL/6 | This paper | In process of depositing at EMMA |
| Mouse: Lmx1bKiZFLARMemMaros Genetic description The zebrafish LARM enhancer (164bp) was introduced twice 5' to LARM2 in the mouse genome. This configuration was not designed but introduced by the CRISPR. The resulting situation is 2 zebrafish enhancers in addition to the normal mouse regulatory region. Current genetic background C57BL/6 | This paper | In process of depositing at EMMA |
| Zebrafish: Lmx1bb_Mmus_LARM1Genetic description: The LARM1 (e + s) region from mouse (*Mus musculus*) was introduced by Tol2-mediated transgenesis in one-cell stage zebrafish embryos. | This paper | The transgenic line will be maintained at the CABD fish facility. Internal ID: Lmx1bb_Mmus_LARM1 |
| Zebrafish: Lmx1bb_Mmus_LARM2 Genetic description: The LARM2 region from mouse (*Mus musculus*) was introduced by Tol2-mediated transgenesis in one-cell stage zebrafish embryos. | This paper | The transgenic line will be maintained at the CABD fish facility. Internal ID: Lmx1bb_Mmus_LARM2 |
| Zebrafish: Lmx1bb_Scan_LARM1 Genetic description: The catshark (*Scyliorhinus canicula*) orthologous region to mouse LARM1e was introduced by Tol2-mediated transgenesis in one-cell stage zebrafish embryos. | This paper | The transgenic line will be maintained at the CABD fish facility. Internal ID: Lmx1bb_Scan_LARM1 |
| Zebrafish: Lmx1bb_Leri_LARM1 Genetic description: The skate (*Leucoraja erinacea*) orthologous region to mouse LARM1e was introduced by Tol2-mediated transgenesis in one-cell stage zebrafish embryos. | This paper | The transgenic line will be maintained at the CABD fish facility. Internal ID: Lmx1bb_Leri_LARM1 |
| Zebrafish: Lmx1bb_Xtro_LARM1 Genetic description: The xenopus (*Xenopus tropicalis*) orthologous region to mouse LARM1s was introduced by Tol2-mediated transgenesis in one-cell stage zebrafish embryos. | This paper | The transgenic line will be maintained at the CABD fish facility. Internal ID: Lmx1bb_Xtro_LARM1 |
| Zebrafish: Lmx1bb_Drer_LARM1 Genetic description: The zebrafish (Danio rerio) orthologous region to mouse LARM1 (e + s) was introduced by Tol2-mediated transgenesis in one-cell stage zebrafish embryos. | This paper | The transgenic line will be maintained at the CABD fish facility. Internal ID: Lmx1bb_Drer_LARM1 |
| Zebrafish: Lmx1bb_Drer_LARM1s Genetic description: The zebrafish (*Danio rerio*) orthologous region to mouse LARM1s was introduced by Tol2-mediated transgenesis in one-cell stage zebrafish embryos. | This paper | The transgenic line will be maintained at the CABD fish facility. Internal ID: Lmx1bb_Drer_LARM1s |
| Zebrafish: Lmx1bb_Drer_LARM1sTandem Genetic description: The zebrafish (*Danio rerio*) orthologous region to mouse LARM1s was introduced twice, in tandem, by Tol2-mediated transgenesis in one-cell stage zebrafish embryos. | This paper | The transgenic line will be maintained at the CABD fish facility. Internal ID: Lmx1bb_Drer_LARM1sTande m |

(*Continued on next page*)

Please cite this article in press as: Hawkins et al., The origin and evolution of dorsal determination mechanisms in vertebrate paired appendages, Current Biology (2026), https://doi.org/10.1016/j.cub.2026.05.046





*Continued*

| REAGENT or RESOURCE | SOURCE | IDENTIFIER |
|---|---|---|
| Zebrafish: Lmx1bb_Hsap_LARM1 Genetic description: The human (*Homo sapiens*) orthologous region to mouse LARM1 (e + s) was introduced by Tol2-mediated transgenesis in one-cell stage zebrafish embryos. | This paper | The transgenic line will be maintained at the CABD fish facility. Internal ID: Lmx1bb_Hsap_LARM1 |
| Zebrafish: Lmx1bb_Hsap_LARM2 Genetic description: The human (*Homo sapiens*) orthologous region to mouse LARM2 was introduced by Tol2-mediated transgenesis in one-cell stage zebrafish embryos. | This paper | The transgenic line will be maintained at the CABD fish facility. Internal ID: Lmx1bb_Hsap_LARM2 |
| Zebrafish: Lmx1bb_Nfor_LARM1 Genetic description: The Australian lungfish (*Neoceratodus forsteri*) orthologous region to mouse LARM1s was introduced by Tol2-mediated transgenesis in one-cell stage zebrafish embryos. | This paper | The transgenic line will be maintained at the CABD fish facility. Internal ID: Lmx1bb_Nfor_LARM1 |
| Zebrafish: Lmx1bb_Nfor_LARM2 Genetic description: The Australian lungfish (*Neoceratodus forsteri*) orthologous region to mouse LARM2 was introduced by Tol2-mediated transgenesis in one-cell stage zebrafish embryos. | This paper | The transgenic line will be maintained at the CABD fish facility. Internal ID: Lmx1bb_Nfor_LARM2 |
| Zebrafish: Lmx1bb_Arut_LARM1 Genetic description: The sterlet (*Acipenser rutheus*) orthologous region to mouse LARM1e was introduced by Tol2-mediated transgenesis in one-cell stage zebrafish embryos. | This paper | The transgenic line will be maintained at the CABD fish facility. Internal ID: Lmx1bb_Arut_LARM1 |
| Zebrafish: Lmx1bb_Arut_LARM2 Genetic description: The sterlet (*Acipenser rutheus*) orthologous region to mouse LARM2 was introduced by Tol2-mediated transgenesis in one-cell stage zebrafish embryos. | This paper | The transgenic line will be maintained at the CABD fish facility. Internal ID: Lmx1bb_Arut_LARM2 |
| Zebrafish: lmx1ba exon 2 frameshift null | This paper | Internal ID: mh296 Deposition pending at Cryogenetics |
| Zebrafish: lmx1bb exon 3 frameshift null | This paper | Internal ID: mh297 Deposition pending at Cryogenetics |
| Zebrafish: en1a exon 1 ATG deletion null | This paper | Internal ID: mh298 Deposition pending at Cryogenetics |
| Zebrafish: en1b exon 1 frameshift null | This paper | Internal ID: mh299 Deposition pending at Cryogenetics |
| Zebrafish: del(LARM1s) | This paper | Internal ID: mh300 Deposition pending at Cryogenetics |
| Zebrafish: del(LARM1e) | This paper | Internal ID: mh306 Deposition pending at Cryogenetics |
| Zebrafish: del(LARM1) | This paper | Internal ID: mh307 Deposition pending at Cryogenetics |
| Zebrafish: del(LARM2) | This paper | Internal ID: mh305 Deposition pending at Cryogenetics |
| Zebrafish: del(holoLARM) | This paper | Internal ID: mh301 Deposition pending at Cryogenetics |
| Oligonucleotides | | |
| See Table S1 | This paper | N/A |
| Software and algorithms | | |
| CHOPCHOP | Montague et al.[40] | https://chopchop.cbu.uib.no |
| PhastCons | Siepel et al.[41]; Hubisz et al.[42] | http://compgen.cshl.edu/phast/ |
| R | R Core Team[43] | http://www.R-project.org/ |
| UCSC Genome Browser | Perez et al.[44] | http://genome.ucsc.edu |
| Jalview | Waterhouse et al.[45] | https://www.jalview.org/ |

(*Continued on next page*)

Please cite this article in press as: Hawkins et al., The origin and evolution of dorsal determination mechanisms in vertebrate paired appendages, Current Biology (2026), https://doi.org/10.1016/j.cub.2026.05.046



*Continued*

| REAGENT or RESOURCE | SOURCE | IDENTIFIER |
|---|---|---|
| VISTA | Dubchak et al.[46]; Frazer et al.[47] | https://genome.lbl.gov/vista/index.shtml |
| Progressive Cactus | Armstrong et al.[48] | 10.5281/zenodo.3873410 |
| FIMO | Sandelin et al.[49] | https://meme-suite.org/meme/doc/fimo.html |
| Other | | |
| Alt-R CRISPR-Cas9 tracrRNA | IDT | Cat# 1072533 |
| Alt-R S.p. Cas9 Nuclease V3 | IDT | Cat# 1081058 |

## EXPERIMENTAL MODEL AND STUDY PARTICIPANT DETAILS

### Mouse husbandry

Mouse husbandry and use were conducted according to the EU regulations and 3R principles, reviewed and approved by the Bioethics Committee of the University of Cantabria. All strains were maintained in a C57BL/6J background and comparable numbers of male and female individuals were observed in each experiment. We did not detect a sex bias in the phenotypes reported in this paper.

### Fish husbandry

All experiments involving zebrafish (*Danio rerio*) performed in this work conform to European Community standards for the use of animals in experimentation and were approved by the Ethical Committees from the Universidad Pablo de Olavide and the Andalusian Government, or Institutional Animal Care and Use Committee (IACUC) of Boston Children's Hospital. Wild-type and genetically modified zebrafish (mutants and transgenics) were maintained and bred under standard conditions following Aleström et al.[50] Embryos were staged in hours and days post-fertilization (hpf and dpf, respectively) as previously described by Kimmel et al.[51] CRISPR experiments were performed in the T5D background and transgene assays were conducted in the AB and Tu backgrounds. Lamprey (*Petromyzon marinus*) care and experiments were approved by the IACUC of the University of Colorado at Boulder under protocol 2392.

## METHOD DETAILS

### Hybridization chain reaction

Zebrafish: HCR RNA-FISH technique was performed in zebrafish following the official protocol by Molecular Instruments (https://files.molecularinstruments.com/MI-Protocol-RNAFISH-Zebrafish-Rev11.pdf) and Choi et al.[52] for whole-mount embryos and larvae. Zebrafish embryos were collected at the desired stages, fixed in 4% paraformaldehyde in phosphate buffered saline (PBS) overnight at 4°C and then washed with PBS to stop the fixation. Subsequently, they were dehydrated through an increasing series of methanol (MeOH) solutions in PBS, for their final storage in 100% MeOH at -20°C. Before use, embryos were rehydrated in an inverse series of MeOH/PBST. Juveniles at 14 dpf were permeabilized by incubating them for 7 minutes in a solution containing 10 μg of proteinase K in PBS.

This step was skipped for embryos at 31, 36, 48 and 56 hpf. Then they were incubated in a pre-hybridization buffer at 37°C, followed by the addition of specific pairs of DNA probes and overnight incubation at same temperature. Afterwards, washes were performed to remove unbound probes, and the fluorescent signal was triggered and amplified using fluorophore-associated pair of hairpins. Finally, the embryos were washed to remove the excess of hairpins and stained with DAPI to be visualized in a confocal microscope Leica Stellaris 5. Buffers and hairpins were ordered from Molecular Instruments, Inc. DNA probes targeting *lmx1bb*, *wnt7aa*, *en1a*, *lbx1b*, and *pax3a* were designed according to Elagoz et al.,[53] synthesized as oPools (IDT), and used in combination with hairpin amplifiers from Molecular Instruments. The sequences used for probe design are provided in Table S1. Mouse: Detection of *Lmx1b* and *En1* transcripts in embryonic mouse limbs was performed following the "Optimized protocol for whole-mount RNA fluorescent in situ hybridization using oxidation-mediated autofluorescence reduction on mouse embryos" described by Morabito et al.[54] Probe sets targeting *Lmx1b* (NM_010725.3) and *En1* (NM_010133.2) were obtained from Molecular Instruments, along with-corresponding B3 and B4 hairpin amplifiers conjugated to Alexa Fluor 647 and Alexa Fluor 488, respectively. Fluorescent images were acquired using a Leica SP5 confocal microscope.

### Allele generation in zebrafish with CRISPR-Cas9

Null alleles of *en1a*, *en1b*, *lmx1ba*, and *lmx1bb* were generated by inducing start codon-deleting mutations or frameshift lesions early in the coding region of each gene using CRISPR-Cas9. Guides were designed using CHOPCHOP[40,55] and synthesized as crRNAs and used with the Alt-R platform (IDT). Gene-specific crRNAs were duplexed with tracrRNA to a final concentration of 6.25 μM with

Please cite this article in press as: Hawkins et al., The origin and evolution of dorsal determination mechanisms in vertebrate paired appendages, Current Biology (2026), https://doi.org/10.1016/j.cub.2026.05.046





1 μg Alt-R S.p. Cas9 nuclease V3 (IDT). This mix was microinjected into T5D strain zebrafish embryos at the one-cell stage. Targeting efficiency was estimated using the T7 endonuclease assay[56] and injected embryos were raised to adulthood. Injected individuals were outcrossed to wild type animals to recover germline loss-of-function alleles. Genotyping primer and guide sequences are reported in Table S1 and mutant line information is given in the key resources table.

Enhancer deletion lines removing the zebrafish *LARM* elements were generated using pairs of CRISPR-Cas9 guides flanking the targeted interval to be removed. CHOPCHOP[40,55,57] was used to design guides in the zebrafish *LARM* region (Table S1). RNP complexes for each individual guide were assembled as described above and mixed at a 1:1 ratio with their mate guide and microinjected as pairs into single cell T5D zebrafish embryos at a final concentration of 6.25 μM with 1 μg Alt-R S.p. Cas9 Nuclease V3 (IDT). Injected clutches were screened by deletion-spanning PCR to detect successful removal. Injected embryos were raised to adulthood and outcrossed to wild type fish, and deletion-spanning PCR was used to identify carriers of the desired deletion. The 164 bp *LARM1s* element was targeted using guides zfLARM_g1 and zfLARM_g2 and deletion was detected by primers zfLARM1s_F and zfLARM1s_R. The *LARM1e* element was targeted using guides zfLARM_g1 and zfLARM_g3 and the deletion was detected by primers zfLARM1e_F and zfLARM1e_R. The *LARM1* element was targeted using guides zfLARM_g3 and zfLARM_g6 and the deletion was detected by primers zfHoloLARM_F and zfLARM_R. The *LARM2* element was targeted using guides zfLARM_g4 and zfLARM_g5 and the deletion was detected by zfLARM2_F and zfLARM2_R. The holo-*LARM* was targeted by guides zfLARM_g3 and zfLARM_g4 and the deletion was detected by primers zfHoloLARM_F and zfHoloLARM_R. The recovered allele of the *LARM1s* deletion carries a clean 188 bp deletion of the targeted element, removing the interval chr8:33401833-33402020 (GRCz11). The recovered holo-*LARM* allele removes the 6,845 bp interval between chr8:33400177-33407021 (GRCz11) and replaces it with the 8 bp scar 'ACTTACTT,' a motif found within the zfLARM_g4 sequence. The recovered *LARM2* allele is a clean deletion of the interval chr8:33406257-33407020 (GRCz11). The recovered *LARM1e* deletion removes the interval between chr8: 33400176-33401832 (GRCz11) and replaces it with the 39 bp scar 'TTGGATTTTGTAACTACATCTGACCACTAAAGCCTTCAG.' The *LARM1* deletion cleanly removes the interval between chr8:33400181-33402868. Genotyping PCR primers are listed in Table S1, and mutant line information is given in the key resources table. The phenotypes reported for each stable mutant zebrafish line are based on a minimum of 10 individuals and were consistent within each genotypic class.

## Mouse strains

C57BL/6J wildtype mice, *ΔLARM1/2*,[1] *zfLARM*, and *zfLARM-355* mutant mouse lines were used in this study. All strains were maintained in a C57BL/6J background. The *zfLARM and zfLARM-355* mutants were generated using CRISPR-Cas9 mediated genome editing. To replace the mouse *LARM* region with the zebrafish *LARM1s* ortholog, we used the two gRNAs (355 and 372) described in Haro et al.[1] (Table S1) which flank the *LARM1* and *LARM2* mouse elements (chr2:33699834-33707488, mm10). This regulatory region of the *Lmx1b* gene was replaced by homology directed repair (HDR) using a 500-nt single-stranded DNA (ssDNA) donor containing the 164-nt zebrafish *LARM1s* enhancer flanked by 168-nt homology arms corresponding to the 5′ and 3′ deletion breakpoints. The donor sequence was synthesized by GenScript® (GenExactTM ssDNA) and is provided in Table S1. The zfLARM-355 transgenic line resulted from an unintended CRISPR-Cas9 event, leading to the insertion of two zebrafish *LARM1s* elements in opposite orientations at the 355-gRNA target site. All primers used for genotyping the mutant lines are listed in Table S1. To genotype the *ΔLARM1/2* deletion, PCR with the 335_Fwd and 335_Rev primers produces a 361 bp product from the wild-type allele, and PCR with the 372_Far_Fwd and 355_Far_Rev primers yields a ∼1.5 kb band in the deletion allele. Genotyping the *zfLARM1sKi* allele was performed with the 355_Fwd and 355_Rev primers that amplify a 361 bp band from the wild-type allele and a 553 bp band from the knockin allele. To detect the *355-zfLARMKi* allele, PCR with the ZF_Fwd and 355_Far_Rev primers will make a 930 bp band in the mutants.

## Skeletal staining

Zebrafish: Adult zebrafish were euthanized by tricaine overdose and fixed overnight in 3.7% formaldehyde in phosphate buffered saline (PBS) at room temperature with agitation. After fixation, specimens were washed in PBS for one hour, then dehydrated through a stepped series of 2-hour washes of graded ethanol series into 100% ethanol. Following dehydration, animals were stained in Alcian Blue (70% ethanol, 30% acetic acid, 0.015% Alcian Blue) overnight at room temperature with rocking. After staining specimens were washed in 95% ethanol for 1 hour and then rehydrated through a stepped series of 2-hour washes of ethanol, and then washed in tap water twice for 1 hour each. Rehydrated specimens were then macerated in trypsin solution (0.3% bovine trypsin powder in 65% saturated sodium borax solution) for 90 minutes at 37°C. Specimens were then stained overnight in Alizarin solution (0.25% in 0.5% potassium hydroxide (KOH) solution) at room temperature with agitation. Specimens were washed in 0.5% KOH for 1 day and then moved into 100% glycerol. Mouse: Limbs from 1-month-old mice were collected, skinned, and fixed overnight in 95% ethanol. For cartilage staining, samples were incubated in Alcian Blue solution (80% ethanol, 20% glacial acetic acid, and 0.3 mg/ml Alcian Blue) for 48–72 hours, then rinsed twice in 95% ethanol for 1–2 days. Limbs were subsequently cleared in 1% potassium hydroxide (KOH) for 24 hours or until the skeletal elements became visible. Bone staining was performed by incubating samples in 0.05 mg/ml Alizarin Red in 1% KOH, in the dark, for 24–48 hours. Following staining, samples were cleared in 20% glycerol/1% KOH for 24 hours and then dehydrated through a graded series of 70% ethanol:glycerol:water mixtures (1:2:7;3:3:4; 4:4:2; 5:5:0). Finally, skeletal preparations were photographed and stored in 70% ethanol:glycerol:water (5:5:0).

Please cite this article in press as: Hawkins et al., The origin and evolution of dorsal determination mechanisms in vertebrate paired appendages, Current Biology (2026), https://doi.org/10.1016/j.cub.2026.05.046



### Analysis of Hi-C data

To analyze the conservation of the *Lmx1b* 3D genome architecture we used publicly available Hi-C data from pectoral fins of stage 30 skate embryos,[58] 48 hpf zebrafish embryos,[59] and limb buds of E11.5 mice.[60] The chromatin contacts within the *Mvb12b-Zbtb34/43* locus were visualized in the UCSC Genome Browser[44] (http://genome.ucsc.edu).

### Identification of *LARM* ortholog sequences in fishes

We generated a hidden Markov model (HMM) for deep sequence homology using 'nhmmer' following Wheeler and Eddy[61] to look for homologous regions in vertebrate genomes. We selected 12 species including mammals, birds, one reptile and one lobe-finned fish (chicken, turkey, coelacanth, human, bat, whale, cow, manatee, otter, seal, gecko, and mouse) based on the high quality annotation of the syntenic region of interest (*Mvb12b-Lmx1b*). The *LARM* sequences of the mentioned species were retrieved using a blastn query with the mouse *LARM* elements (*LARM1s* chr2:33701467- 33701677; *LARM1e* chr2:33700794-33701108; *LARM2* chr2:33705926-33706432; mm10 coordinates). Then, we performed a Multiple Sequence Alignment (MSA) using clustalw2[62] with the default parameters for DNA sequences, and this MSA was used to generate an HMM profile using 'hmbuild' from HMMER.[61] The database for homology searching consists in a multi FASTA file containing the genomic region around the *Lmx1b* gene spanning 30 times the length of their annotated *Lmx1b* of different fish species (skate, catshark, spotted gar, sterlet sturgeon, zebrafish, medaka, coelacanth, and Australian lungfish). This length was arbitrary defined with the idea of covering the *Lmx1b* regulatory landscape where the *LARM* elements are contained.

To identify additional *LARM* elements across gnathostome evolution potentially missed by the lobe-finned fish-based model, we generated an additional model using the same methodology but using sequence from ray-finned fishes. We selected 11 species representing key lineages distributed across actinopterygian phylogeny (reedfish, sterlet, spotted gar, Atlantic tarpon, European eel, Asian bonytongue, zebrafish, haddock, fugu, Japanese flounder, and medaka). *LARM* element sequences from these species were retrieved using blastn with the zebrafish *LARM* elements (*LARM1s* chr8: 35511073-35511507; *LARM1e* chr8:35510830-35510981; *LARM2* chr8: 35515495-35515963 from the GRCz12tu assembly). *LARM* element sequences and genomic location information are provided in Table S2.

### Enhancer reporter assays in zebrafish

Transgenic embryos were generated using the Tol2 transposase system.[63] The sequences of assayed *LARM* elements are provided in Table S2, and the primers used to amplify them are given in Table S1. Putative *LARM* regulatory regions were amplified from genomic DNA by PCR, except for lungfish and sterlet elements, as well as the zebrafish *LARM1s*, which were synthetized by Genewiz (Azenta Life Sciences). PCR products were purified with the Isolate II PCR and Gel Kit (BIOLINE) and cloned into an intermediate vector (pCR8/GW/TOPO, Invitrogen, #10532893). Using Gateway® technology (LR Clonase® II Enzyme mix, Invitrogen, ThermoFisher Scientific), amplicons were finally recombined into an enhancer detection vector containing the *gata2* minimal promoter and the strong midbrain *irx* enhancer *z48* for an internal control of the transgenesis experiment.[64,65] The *z48* enhancer serves as an injection control and also facilitates chromatin opening, acting as a booster for weak enhancers driving GFP expression. To deliver constructs, one-cell stage embryos were microinjected with 2-3 nL of a solution containing 30 ng/μl of transposase mRNA, 20 ng/μL of purified enhancer construct, and 0.05% phenol red solution. The $F_0$ injected embryos were monitored at 24, 48, and 72 hpf for GFP expression (midbrain control and enhancer-specific). GFP+ embryos with enhancer activity in the pectoral fins were raised to sexual maturity and crossed with wildtype animals to obtain $F_1$ animals. The $F_1$ with fin enhancer activity were crossed with wildtype animals, raised and the $F_2$ descendants carrying the enhancer construct were considered as stable transgenic lines. An enhancer was considered to have verified activity in pectoral fins when three or more independent stable transgenic lines from the same construct exhibit similar and consistent expression patterns in the fin. Transgenic embryos were imaged using an Olympus SZX16 fluorescence stereoscope and photographed with an Olympus DP71 camera.

### Whole-mount colorimetric *in situ* hybridization

Zebrafish: The detection of reporter-derived GFP transcripts was performed according to Jowett and Lettice.[66] Briefly, GFP transgenic zebrafish embryos were fixed at the appropriate developmental stage and dehydrated in a Methanol/PBS increasing series. Embryos were rehydrated in a reverse Methanol/PBS-Tween series, prehybridized in hybridization buffer and finally hybridized overnight with 2 ng/μl of the GFP digoxigenin-labeled RNA probe at 70°C. The excess of probe was washed with a decreasing formamide buffers series to reduce the unbound probe background. Embryos were blocked and incubated with the anti-digoxigenin-Alkaline Phosphatase (AP) conjugated antibody solution. AP activity was finally revealed using a staining solution of NBT-BCIP.

Mouse: Mouse embryos were fixed in PFA 4% ON at 4°C, washed in PBS, in PBT (0.1% Tween-20 in PBS), and dehydrated with MeOH by increased concentrations until 100% MeOH. Next day, samples were rehydrated, washed in PBT and bleached with 6% $H_2O_2$/PBT for 1h. Embryos were washed in PBT and digested with Proteinase K (PK, Roche, #03115879001) at 10 μg/ml in PK buffer (50 mM Tris-HCl pH 7.4, 5 mM EDTA), adjusting the digestion time to the embryonic stage. Then, embryos were quickly washed in PBT and post-fixed in 0.25% glutaraldehyde in 4% PFA during 20 min, and leaved in the hybridization buffer at 65°C ON (50% formamide, 5x SSC (saline-sodium citrate), 2% blocking powder, 0.1% Triton X-100, 0.1% CHAPS, 1 mg/ml tRNA, 50 μg/ml Heparin pH 4.5, 500 mM EDTA pH 8). The following day, embryonic samples were frozen at -20°C for at least 6 h, and later incubated with the hybridization buffer containing the desired antisense RNA probe. The next day, several post-hybridization washes (65°C) were carried out to remove nonspecific binding: 3X 2xSSC/0.1% CHAPS 30 min each, and 3X 0.2xSSC/0.1% CHAPS (20-20-30 min). Then,

Please cite this article in press as: Hawkins et al., The origin and evolution of dorsal determination mechanisms in vertebrate paired appendages, Current Biology (2026), https://doi.org/10.1016/j.cub.2026.05.046



samples were washed twice with KTBT buffer (50 mM Tris- HCl pH 7.4, 150 mM NaCl, 10 mM KCl, 1%Triton X-100) for 10 min at RT, and later blocked in 20% sheep serum/KTBT for 2 h at RT. Embryos were incubated with Anti-Digoxigenin-AP (Roche, #11093274910) diluted 1:2,000 in blocking solution at 4°C ON. After this, several washes were performed with KTBT at RT. Finally, signal detection was performed by incubating the embryos in darkness in NTMT buffer (100 mM Tris-HCl pH 9.5, 50 mM MgCl2, 100 mM NaCl, 1% Triton X-100), with NBT (3 μg/ml) and BCIP (2.3 μg/ml) substrates. Once the desired signal level was reached, reaction was stopped with several washes in KTBT and fixed in 4% PFA for photographing.

Lamprey: Two *Lmx1b* genes are annotated in the kPetMar1.pri Feb. 2020 sea lamprey genome assembly (GCF_010993605.1), one on chromosome 59 (XM_032976538.1) which we have called *Lmx1bα* and the other on chromosome 22 (XM_032959033.1) which we have called *Lmx1bβ*. To generate *in situ* hybridization probe templates, we ordered from GENEWIZ/Azenta synthesized DNA fragments corresponding to exon-spanning segments of either transcript flanked by Sp6, T7, and M13 primer sites (Table S1). These templates were used to synthesize digoxigenin-labelled RNA probes as previously described.[67] Embryonic and larval material was obtained as in Cattell et al.[68] and animals were staged according to Tahara.[69] Whole-mount *in situ* hybridization was performed following Meulemans and Bronner-Fraser[70] with the modification that proteinase K treatment for 6 cm ammocete larvae for 20 minutes at a concentration of 1.6 IU/mL in PBST.

### Immunolabelling of pectoral fin musculoskeletal elements

Immunolabelling was performed using a skeletal muscle antibody (12/101, Developmental Studies Hybridoma Bank) and anti-thrombospondin 4 antibody (Abcam). The labelling protocol followed the Deepclear method,[71] with several modifications, including an overnight clearing in solution 1.1, primary antibody incubation for 3 days at 37°C, incubation in the secondary for two days at room temperature, and a five-minute incubation in alizarin red S for bone counterstaining, with a final clearing step using methanol dehydration, followed by dichloromethane incubation and methyl cinnamate. Images were taken at 20x using a Leica Stellaris confocal microscope. Scans were segmented such that dorsal hemirays are labeled blue, ventral hemirays are labeled red, and the shoulder is labeled magenta.

### Micro computed tomography (μCT)

Limbs from 1-month-old mice were scanned using a Skyscan 1172 micro-CT scanner (Bruker) at 40 kV, 100 μA, and a pixel resolution of 27.0 μm. Image reconstruction was performed using NRecon software (Bruker), and 3D renderings were generated with CTvox v3.3.1 (Bruker).

### VISTA genome alignments

To identify conserved *LARM* elements, the *Mvb12b-Lmx1b* intergenic region from different species were aligned using mVISTA[46,47] (https://genome.lbl.gov/vista/index.shtml). Sequences were aligned using default parameters and the LAGAN alignment program.[72]

### 3D Reconstruction of cypriniform pectoral fin skeletons

All cypriniform computed microCT data sets were accessed on MorphoSource[73] (www.morphosource.org). The ARK identifiers and specimen information are listed in Table S4. Access to these open-source data was provided with support from oVert TCN, NSF DBI-1701753, and NSF DBI-1701714. Reconstructions were down sampled to 8-bit and cropped to the pectoral fin region of interest using ImageJ.[74] Processed reconstructions were visualized and imaged in Amira 6 (FEI Systems).

### Loach material and analysis of *LARM1e* element in hillstream loaches

Individuals of *Misgurnus anguillicaudatus* and *Sewellia lineolata* were obtained through the commercial aquatic trade and euthanized for anatomical and genomic analyses. To verify the *LARM1e* deletions in the *Beaufortia* genomic data, we cloned this region from *Sewellia lineolata* using using PCR with the primers LARM1e_F and LARM1e_R (Table S1).

### SEM imaging of fin tubercles

Wild type and homozygous $LARM^{\Delta 6.8\ kb}$ deletion mutant fins were fixed overnight in 3.7% formaldehyde in PBS overnight at room temperature with agitation. After fixation, specimens were rinsed in PBS for one hour and then moved through a graded series into 100% ethanol, and washed in 100% ethanol several times to ensure dehydration. Following dehydration, fins were subjected to critical point drying and then directly mounted on SEM specimen stubs without coating. Fins were imaged using a JEOL JSM-6010 LV Scanning Electron Microscope.

### Spawning performance trials

10 homozygous holo-*LARM* deletion mutant males and 10 wildtype sibling males were mated with two groups (group A and group B) of 10 wildtype T5D females each. Animals were mated four times with one-week intervals between each spawning trial and were not set up for other crosses for the duration of the experiment.

Matings were conducted as individual male and female pairs (one pair per spawning arena). On week 1 mutant males were paired with group A females and wildtype males were paired with group B females, and females were alternated between males each following (for example, on week 2 mutant males were paired with group B females). Mating pairs were set up in the evening and eggs were collected the following morning, and the number of successful spawns and each clutch size were recorded.

Please cite this article in press as: Hawkins et al., The origin and evolution of dorsal determination mechanisms in vertebrate paired appendages, Current Biology (2026), https://doi.org/10.1016/j.cub.2026.05.046



### Evolutionary rate analysis of cypriniform *LARM* elements

To characterize the *LARM* region across order Cypriniformes, we used BLAST+ v2.14.1 (Camacho et al.[75]) to identify sequences orthologous to *LARM1* across a series of cypriniform genomes: *Barbatula barbatula* (GCA_037178815.1), *Beaufortia kweichowensis* (GCA_019155185.1), *Beaufortia pingi* (GCA_044048495.1), Carassius gibelio (GCA_023724105.1), *Chromobotia macracanthus* (GCA_036877525.1), *Ctenopharyngodon idella* (GCF_019924925.1), *Danio rerio* (GCF_049306965.1), *Gobio gobio* (GCA_949357685.1), *Leptobotia elgongata* (GCA_039881065.1), *Leuciscus chuanchicus* (GCA_965140175.1), *Misgurnus anguillicaudatus* (GCF_027580225.2), *Myxocyprinus asiaticus* (GCF_019703515.2), *Triplophysa yaopeizhii* (GCA_048296945.1). For *Carassius gibelio* and *Myxocyprinus asiaticus*, which have undergone recent, independent whole-genome duplications, we included both orthologous *LARM* loci.

Each identified *LARM* locus was extended by 250 kilobases (kb) upstream and downstream to create a 500 kb region. These extended loci were aligned using Progressive Cactus v2.9.9 (Armstrong et al.[48]) to generate a multiple genome alignment. The resulting Hierarchical Alignment (HAL) file was converted to a Multiple Alignment File (MAF) using hal2maf (parameters ' –chunkSize 10000—noAncestors –dupeMode single').

The cladogram used in the Cactus alignment and all subsequent analyses was based on Stout et al.,[76] with the exception that Wang et al.[77] was used for the topology within loaches provided its greater sampling of loach lineages. The resulting composite cladogram is:(((((((beaufortia_pingi,beaufortia_kweichowensis),misgurnus_anguillicaudatus),(triplophysa_yaopeizhii, barbatula_barbatula)),(leptobotia_elgongata,chromobotia_macracanthus)),(((leuciscus_chuanchicus,gobio_gobio),ctenopharyngodon_idella),danio_rerio)),(carassius_gibelio,carassius_gibelio2)),(myxocyprinus_asiaticus,myxocyprinus_asiaticus2)).

To identify conserved elements within the intergenic region between *lmx1bb* and *mvb12bb*, we applied PhastCons[41,42] on the 500 kb MAF (PHAST v1.5; parameters ' –target-coverage 0.25 –expected-length 12 –msa-format MAF). Prior to running PhastCons, we generated a phylogenetic model using phyloFit (PHAST v1.5) based on the full 500 kb extended LARM locus. We then calculated a 20 bp sliding window average (with 1 bp step size) of the PhastCons score across the resulting wiggle (WIG) file to identify peaks of conservation. Within these peaks we identified three discrete conserved *LARM* elements: *LARM1e*, *LARM1s*, and *LARM2*. Within each *LARM*, we evaluated coverage and conservation by comparing the sequences of each species to *Danio rerio*. To test for accelerated sequence evolution in these regions, we used phyloP[78] (PHAST v1.5) on each LARM (parameters ' –mode ACC –method LRT –features –subtree').

We assessed the presence or absence of transcription factor binding site motifs across the phylogeny using the Find Individual Motif Occurrences tool[79] (FIMO v5.5.5) and the JASPAR2022 CORE non-redundant database[49]. Motifs that were specifically gained or lost within *Beaufortia* (FIMO q-value < 0.05) in the *LARM1e* region were recorded (Table S5).

## QUANTIFICATION AND STATISTICAL ANALYSIS

Statistical details of experiments are detailed in the legends of the figures in which the relevant results are presented. Parameters of bioinformatics analyses are detailed within each relevant sections of the method details section.